Eur. Phys. J. B **13**, 209–225 (2000)

THE EUROPEAN
PHYSICAL JOURNAL B
EDP Sciences

Perturbation theory by flow equations: dimerized and frustrated S = 1/2 chain

C. Knetter[a] and G.S. Uhrig[b]

Institut für Theoretische Physik, Universität zu Köln, Zülpicher Straße 77, Köln 50937, Germany

Received 5 May 1999 and Received in final form 7 June 1999

Abstract. The flow equation method (Wegner, 1994) is used as continuous unitary transformation to construct perturbatively effective Hamiltonians. The method is illustrated in detail for dimerized and frustrated antiferromagnetic $S = 1/2$ chains. The effective Hamiltonians conserve the number of elementary excitations which are $S = 1$ magnons for the dimerized chains. The sectors of different number of excitations are clearly separated. Easy-to-use results for the gap, the dispersion and the ground state energies of the chains are provided.

PACS. 75.10.Jm Quantized spin models – 02.30.Mv Approximations and expansions – 03.65.-w Quantum mechanics

1 Introduction

Perturbation theory is one of the most important and most versatile tools for problems which are not exactly solvable. Various methods depending on the problem under study have been invented and used. Due to the enormous increase in computer capacity it is a very interesting task to use algebraic programmes to perform perturbative calculations.

The aim of the present work is to propose a general perturbation scheme which splits naturally into two subsequent steps. Both these steps can be implemented in a direct manner on the computer. The first step is not model specific. It relies only on two prerequisites.

(i) The unperturbed Hamiltonian H_0 must have an equidistant spectrum bounded from below. Without loss of generality we may assume that $E_i = i$ for $i \in \{0, 1, 2, 3, \dots\}$. We say that i denotes the number of energy quanta in the system. By U_i the corresponding subspaces are denoted.

(ii) The perturbing Hamiltonian H_S links subspaces U_i and U_j only if $|i - j|$ is bounded from above, *i.e.* there is a number $N > 0$ such that H_S can be written as $H_\text{S} = \sum_{n=-N}^{N} T_n$ where T_n increments (or decrements, if $n < 0$) the number of energy quanta by n

$$[H_0, T_n] = nT_n. \tag{1}$$

Thus the full problem reads

$$H = H_0 + \lambda \sum_{n=-N}^{N} T_n \tag{2}$$

where λ is the perturbation parameter supposed to be small $\lambda < 1$. In this work we will restrict to $N = 2$. The first step consists in finding a systematic mapping of the problem in equation (2) to an effective one given by a Hamiltonian H_eff which conserves the number of energy quanta.

The second step is the model specific one. It consists in the actual calculation of H_eff for a given number of energy quanta.

To illustrate the abstract ideas formulated above we will use the frustrated and dimerized $S = 1/2$ chain given by (j counts the sites)

$$H = J_0 \sum_{j=0}^{L} \left[(1 + (-1)^j\delta)\mathbf{S}_j\mathbf{S}_{j+1} + \alpha_0\mathbf{S}_{j-1}\mathbf{S}_{j+1}\right], \tag{3}$$

where L is the number of sites. A situation consistent with equation (2) is found for strong dimerization. Hence we rewrite Hamiltonian (3) as (subscript i counts the dimers)

$$H = J \sum_{i=0}^{\frac{L}{2}-1} [\mathbf{S}_{2i}\mathbf{S}_{2i+1} + \lambda\mathbf{S}_{2i}\mathbf{S}_{2i-1} + \alpha(\mathbf{S}_{2i}\mathbf{S}_{2i-2} + \mathbf{S}_{2i-1}\mathbf{S}_{2i+1})] \tag{4}$$

---

[a] e-mail: `ck@thp.uni-koeln.de`

[b] e-mail: `gu@thp.uni-koeln.de`

with

$$J = J_0(1+\delta) \tag{5a}$$
$$\lambda = (1-\delta)/(1+\delta) \tag{5b}$$
$$\alpha = \alpha_0/(1-\delta). \tag{5c}$$

The unperturbed part H_0 (up to a trivial constant $3L/8$) and the perturbing part H_S are then

$$H_0 = \sum_i \left[\mathbf{S}_{2i}\mathbf{S}_{2i+1} + 3/4\right] \tag{6a}$$
$$H_\mathrm{S} = \sum_i \left[\mathbf{S}_{2i}\mathbf{S}_{2i-1} + \alpha\left(\mathbf{S}_{2i}\mathbf{S}_{2i-2} + \mathbf{S}_{2i-1}\mathbf{S}_{2i+1}\right)\right], \tag{6b}$$

where we measure implicitly all energies in units of J. The ground state of H_0 is the product of singlets on the dimers, *i.e.* the bonds $(2i, 2i+1)$. The energy quanta are here the excited dimers, namely the local triplets. The number of triplets classifies the degenerate energy eigen spaces of the unperturbed problem.

Besides the purpose to serve as an example for perturbation by flow equations the frustrated and dimerized chain is of considerable physical interest itself. Ideal spin-Peierls systems are one-dimensional spin systems which are coupled to the lattice. At low enough temperatures they dimerize since this dimerization leads to a gain in magnetic energy $\propto \delta^{4/3}$ which overcompensates the loss in elastic energy $\propto \delta^2$, see *e.g.* [1] and references therein. So spin-Peierls systems provide dimerized spin chains in a natural way. The first inorganic spin-Peierls substance $\mathrm{CuGeO_3}$ in particular provides the example of a frustrated and dimerized spin chain since there is much evidence that a certain amount of frustration is present in this substance [2–4]. Other examples are strongly anisotropic substances where the dimerization is built-in in the chemical structure. Examples are $\mathrm{Cu_2(C_5H_{12}N_2)_2Cl_4}$ [5] and $\mathrm{(VO)_2P_2O_7}$ [6]. Of course, the real substance mostly display also some additional two- or three-dimensional coupling. But the approach we present here is suited to tackle even these systems, see *e.g.* reference [7].

One might argue that exact diagonalization or quantum Monte Carlo approaches are better suited to calculate dispersions $\omega(k)$ or similar quantities in $d = 1$. These methods, however, yield only the result for the chosen parameter set. The perturbative results, however, will be obtained as polynomials in the weak bond coupling λ and the frustration α. Thus, once computed, anyone can use the perturbative results easily to fit measured or otherwise obtained data. Thereby an extremely fast method for the determination of coupling constants is provided. Of course, the perturbative approach can be applied only for $\lambda \leq 1$ where the equal sign represents the worst case. For $\lambda > 1$ the perturbative approach breaks down.

The work is organized as follows. In the next section we extend the approach of Stein [8] who did a calculation for $N = 1$ up to fifth order to $N = 2$ and up to tenth order. The work of Stein improved earlier calculations [9] which generated more intermediate terms (see Ref. [8] for discussion). The flow equation transformation which is used by Stein and by us was introduced by Wegner five years ago [10]. In Section 3 we illustrate our method by applying it to a one-dimensional Heisenberg antiferromagnetic $S = 1/2$ chain. The effective one-triplet Hamiltonian is computed. The ground state energy, gaps and dispersion relations are discussed in Section 4. Summary and outlook conclude the main part of our work.

2 Perturbation by flow equations

All what is presented in this section is based only on the fact that the initial problem has the form (2) fulfilling the requirements (i) and (ii) with $N = 2$.

The general idea behind the flow equation approach introduced by Wegner [10] is to perform a *continuous* unitary transformation which makes the problem more easily tractable. Mostly, one tries to make the problem "more diagonal". In our case we will achieve a block diagonal form. A broad field of application is to identify certain quasi-particles for which an effective Hamiltonian can be found. Here, flow equations can be used to implement a renormalization of a given problem on the Hamiltonian level, not only on the level of certain observables or couplings [10–12]. Analogous ideas were suggested parallel by Głazek and Wilson in the form of similarity transformations [13].

In the present work we do not focus on the renormalization properties of the flow equation approach. Following Stein [8], we use them to implement in a systematic way a continuous unitary transformation which maps the perturbed system onto the unperturbed one which is easy to understand.

2.1 General formalism

According to the original idea a running variable ℓ is introduced which parameterizes the continuously evolving Hamiltonian $H(\ell)$. The starting operator is the bare Hamiltonian; the operator at infinity is the desired effective Hamiltonian

$$H(0) = H_0 + \lambda(T_{-2} + T_{-1} + T_0 + T_1 + T_2) \tag{7a}$$
$$H(\infty) = H_\mathrm{eff}. \tag{7b}$$

The unitary evolution is engendered by its antihermitean infinitesimal generator $\eta(\ell)$

$$\frac{\mathrm{d}H(\ell)}{\mathrm{d}\ell} = [\eta(\ell), H(\ell)]. \tag{8}$$

Applying naively Wegner's choice for the generator $\eta(\ell) = [H_0, H(\ell)]$ the resulting differential equations quickly become very messy since the band block diagonal structure of the original problem is lost. By "band block diagonal" we mean the fact that N has a finite value which does not change in the course of the flow $\ell \to \infty$.

We will choose a slightly different infinitesimal generator which allows to keep the band block diagonal structure of the original problem, *i.e.* the parameter N stays 2 for all values of ℓ. The general Hamiltonian $H(\ell)$ can be written as

$$H(\ell) = H_0 + \lambda\Theta(\ell) \tag{9}$$

and the operator $\Theta(\ell)$ links only subspaces U_i and U_j with $|i-j| \leq 2$.

The most general form of $\Theta(\ell)$ is

$$\Theta(\ell) = \sum_{k=1}^{\infty} \lambda^{k-1} \sum_{|\mathbf{m}|=k} F(\ell;\mathbf{m}) T(\mathbf{m}) \tag{10}$$

where $F(\ell;\mathbf{m})$ are real-valued functions for which we will derive nonlinear, but recursive, differential equations below. The other symbols are

$$\mathbf{m} = (m_1, m_2, m_3, \ldots, m_k) \quad \text{with} \tag{11a}$$
$$m_i \in \{0, \pm 1, \pm 2\} \tag{11b}$$
$$|\mathbf{m}| = k \tag{11c}$$
$$T(\mathbf{m}) = T_{m_1} T_{m_2} T_{m_3} \ldots T_{m_k} \tag{11d}$$
$$M(\mathbf{m}) = \sum_{i=1}^{k} m_i. \tag{11e}$$

The vector $\mathbf{m}$ together with the product $T(\mathbf{m})$ encode all possible products of the incrementing (decrementing) operators T_n as defined in equations (1, 2). The infinitesimal generator of our choice reads

$$\eta(\ell) = \sum_{k=1}^{\infty} \lambda^{k} \sum_{|\mathbf{m}|=k} \operatorname{sgn}\big(M(\mathbf{m})\big) F(\ell;\mathbf{m}) T(\mathbf{m}). \tag{12}$$

This choice is very similar to the infinitesimal generator Mielke proposes for band matrices [14]. An adapted version of his proof that such an η leads to (block) diagonality can be found in Appendix A. For the purposes of the present perturbative approach the general proof can be replaced by the observation that the transformation can be performed successfully to all finite orders. This will be shown below.

A short computation shows that substituting $\operatorname{sgn}\big(M(\mathbf{m})\big)$ in equation (12) by $M(\mathbf{m})$ would correspond to the first choice $\eta(\ell) = [H_0, H(\ell)]$. This relies on

$$[H_0, T(\mathbf{m})] = M(\mathbf{m}) T(\mathbf{m}) \tag{13}$$

which is a straightforward generalization of equation (1).

Insertion of the ansätze (10) and (12) into equation (8) leads to

$$\lambda \frac{\mathrm{d}\Theta}{\mathrm{d}\ell} = \lambda[\eta(\ell), \Theta(\ell)] - \sum_{k=1}^{\infty} \lambda^{k} \sum_{|\mathbf{m}|=k} \operatorname{sgn}\big(M(\mathbf{m})\big) F(\ell;\mathbf{m}) [H_0, T(\mathbf{m})]. \tag{14}$$

Comparison of the coefficients for each term $T(\mathbf{m})$ yields then a differential equation for the functions $F(\ell;\mathbf{m})$

$$\frac{\mathrm{d}}{\mathrm{d}\ell} F(\ell;\mathbf{m}) = -|M(\mathbf{m})| F(\ell;\mathbf{m}) + \sum_{\{\mathbf{m}_1,\mathbf{m}_2\}=\mathbf{m}} \Big[\operatorname{sgn}\big(M(\mathbf{m}_1)\big) - \operatorname{sgn}\big(M(\mathbf{m}_2)\big)\Big] F(\ell;\mathbf{m}_1) F(\ell;\mathbf{m}_2). \tag{15}$$

The summation condition $\{\mathbf{m}_1, \mathbf{m}_2\} = \mathbf{m}$ means that one sums over all possible nontrivial breakups of $\mathbf{m}$

$$\begin{array}{lll}
\mathbf{m}_1 = (m_1) & \text{and} & \mathbf{m}_2 = (m_2, \ldots, m_k)\\
\mathbf{m}_1 = (m_1, m_2) & \text{and} & \mathbf{m}_2 = (m_3, \ldots, m_k)\\
\mathbf{m}_1 = (m_1, m_2, m_3) & \text{and} & \mathbf{m}_2 = (m_4, \ldots, m_k)\\
 & \vdots & \\
\mathbf{m}_1 = (m_1, \ldots, m_{k-2}) & \text{and} & \mathbf{m}_2 = (m_{k-1}, m_k)\\
\mathbf{m}_1 = (m_1, \ldots, m_{k-1}) & \text{and} & \mathbf{m}_2 = (m_k).
\end{array} \tag{16}$$

This summation notation will also be used in the following. The starting conditions follow from (7a)

$$F(0;\mathbf{m}) = 1 \quad \text{for} \quad |\mathbf{m}| = 1 \tag{17a}$$
$$F(0;\mathbf{m}) = 0 \quad \text{for} \quad |\mathbf{m}| > 1. \tag{17b}$$

From equations (15, 17) we can deduce a number of relations by induction. First, we see that the functions $F(\ell;\mathbf{m})$ are always real. Furthermore, they obey the two symmetry relations

$$F(\ell; -\overline{\mathbf{m}}) = F(\ell;\mathbf{m}) \tag{18a}$$

$$F(\ell; -\mathbf{m}) = (-1)^{|\mathbf{m}|+1} F(\ell;\mathbf{m}) \tag{18b}$$

where we use the notation

$$\overline{\mathbf{m}} = (m_k, m_{k-1}, \ldots, m_2, m_1). \tag{19}$$

The square bracket in equation (15) ensures that the sum vanishes if $|M(\mathbf{m})| > 2$

$$F(\ell;\mathbf{m}) = 0 \quad \text{for} \quad |M(\mathbf{m})| > 2. \tag{20}$$

For instance, a term generating three energy quanta $M(\mathbf{m}) = 3$ could only be induced from terms with $M(\mathbf{m}_1) = 2$ and $M(\mathbf{m}_2) = 1$ or *vice-versa*. But such combinations are suppressed by the square bracket in equation (15). This observation is at the basis of the preservation of the band block structure [14]. If we had chosen the infinitesimal generator $\eta(\ell)$ in (12) without the signum as it would correspond to Wegner's original suggestion $\eta(\ell) = [H_0, H(\ell)]$ the square bracket in equation (15) would read $[M(\mathbf{m}_1) - M(\mathbf{m}_2)]$ and hence the band structure of the couplings would be destroyed for $\ell > 0$.

For the solution of equation (15) we observe that the first term on the right hand side just generates an exponential prefactor

$$F(\ell;\mathbf{m}) = \exp(-|M(\mathbf{m})|\ell) f(\ell;\mathbf{m}). \tag{21}$$

The rest of the equation (15) is recursive and can thus be directly found by integration beginning from the starting conditions

$$\frac{\mathrm{d}}{\mathrm{d}\ell} f(\ell;\mathbf{m}) = \sum_{\{\mathbf{m}_1,\mathbf{m}_2\}=\mathbf{m}} \mathrm{e}^{(|M(\mathbf{m})| - |M(\mathbf{m}_1)| - |M(\mathbf{m}_2)|)l} \times \left[\operatorname{sgn}\big(M(\mathbf{m}_1)\big) - \operatorname{sgn}\big(M(\mathbf{m}_2)\big)\right] f(\ell;\mathbf{m}_1) f(\ell;\mathbf{m}_2). \tag{22}$$

Note that $|M(\mathbf{m})| - |M(\mathbf{m}_1)| - |M(\mathbf{m}_2)| \leq 0$ holds so that no exponential growth occurs in the $f(\ell;\mathbf{m})$. Let us focus on the functional form of the functions $f(\ell;\mathbf{m})$. We state by induction that sums of terms $\ell^i \mathrm{e}^{-2\mu\ell}$ occur for non-negative integers i and μ. More precisely, we obtain

$$f(\ell;\mathbf{m}) = \sum_{\mu=0}^{\Gamma(\mathbf{m})} P_\mu(\ell;\mathbf{m})\mathrm{e}^{-2\mu\ell} \tag{23}$$

where the degree of the polynomials $P_\mu(\ell;\mathbf{m})$ is always equal or less than $|\mathbf{m}|$ and the upper limit of the sum $\Gamma(\mathbf{m})$ obeys

$$\Gamma(\mathbf{m}) = \frac{1}{2}\left(-|M(\mathbf{m})| + \sum_{i=1}^{|\mathbf{m}|}|m_i|\right). \tag{24}$$

In principle it is also possible to write down explicit recursion relations for the polynomials, see for instance reference [8] for $N = 1$. But they are of little clarity. If the actual calculation is done by symbolic calculation it is sufficient to retain that according to equation (15) or equation (22) expressions of the type (23) have to be multiplied, added and integrated. This is a straightforward task and can be implemented in symbolic programmes.

The quantities we are finally interested in are the coefficients of $H_{\text{eff}} = H(\ell = \infty)$. From equation (21) we know that only terms with $M(\mathbf{m}) = 0$ will not vanish for $\ell \to \infty$. This is exactly what we intended to achieve since we want H_{eff} to commute with H_0 (*cf.* Eq. (13)) so that the number of energy quanta (triplets in our example) becomes a conserved quantity. Hence, we can write the final result as

$$H_{\text{eff}} = H_0 + \sum_{k=1}^{\infty}\lambda^k \sum_{|\mathbf{m}|=k, M(\mathbf{m})=0} C(\mathbf{m})T(\mathbf{m}) \tag{25a}$$

$$C(\mathbf{m}) = F(\infty;\mathbf{m}). \tag{25b}$$

Further details on the computation of the coefficients will be given in the next subsection. Results for the $C(\mathbf{m})$ are presented in Appendix B.

2.2 Computer aided evaluation

We implemented the coefficient computation in C++ because of its high performance and its class concept which we used to encode the basic data elements. As an example let us consider a generic fourth order coefficient (*i.e.* $k = 4$) $f(l;\mathbf{m})$:

$$f\big(l;(1,1,1,-2)\big) = \frac{1}{2}l + \frac{1}{2}\mathrm{e}^{-2l} - \frac{1}{8}\mathrm{e}^{-4l} - \frac{3}{8}\cdot \tag{26}$$

This can be stored as a list of basic data elements like

$$\frac{p}{q}l^i\mathrm{e}^{-2\mu l} \tag{27}$$

each containing four separate integers p, q, i, μ. In fact, p and q can become very large. So they have to be stored in a multiprecision data type like long long int on some Unix systems. Still, all computations can be done very fast in integers and the results are rigorously exact.

Equation (22) is essential in the computation of the $f(l;\mathbf{m})$. The basic idea is to build two loops. The outer loop controls the order starting at $k = 2$ since the initial conditions are the values of the $f(l;\mathbf{m})$ in first order. The inner loop generates all possible $\mathbf{m}$ in the current order k. A single m_i in $\mathbf{m} = (m_1, \ldots, m_i, \ldots, m_k)$ can take five different values, see equation (11b). Thus we can introduce the loop variable $n \in \{0, 1, \ldots 5^k - 1\}$

$$n = \sum_{i=0}^{5} a_i 5^i. \tag{28}$$

The coefficients $a_i \in \{0, 1, 2, 3, 4\}$ are mapped uniquely onto the set $\{-2, -1, 0, 1, 2\}$. Finally we retain those $\mathbf{m}$, with $|M(\mathbf{m})| \leq 2$. In this way, equation (22) can be calculated for each k and $\mathbf{m}$.

The calculation of a single $f(l;\mathbf{m})$ *via* equation (22) can be split in four steps. (i) One has to encapsulate equation (22) in yet another loop controlling all possible breakups of $\mathbf{m}$ (*cf.* Eq. (16)). (ii) The functions $f(l;\mathbf{m}_1)$ and $f(l;\mathbf{m}_2)$ known from calculations in lower orders have to be multiplied for each breakup of $\mathbf{m}$. (iii) One has to sum over all breakups. (iv) Finally, the result from steps (i) to (iii) has to be integrated.

Since p and q in the basic data elements (27) can become very large during addition and multiplication, both operations employ Euklid's algorithm to generate maximally canceled fractions p/q. To minimize memory usage these operations contain simplification subroutines based on the quick-sort algorithm. These subroutines sort according to increasing powers of l and e^{-2l}. Simultaneously, addends are identified and added if they are of equal type. The resulting $f(l;\mathbf{m})$ consists of linearly independent addends only. Due to the quick-sort algorithm the computation time as function of the number of addends n is only of order $n\ln(n)$.

The final integration can be done easily. The functions $f(l;\mathbf{m})$ break down to basic data elements (27) so that ($\alpha > 0$)

$$\int_0^l \mathrm{d}l' l'^i = \frac{1}{i+1}l^{i+1} \tag{29a}$$

$$\int_0^l \mathrm{d}l' l'^i \mathrm{e}^{-\alpha l'} = \frac{i!}{\alpha}\cdot\left\{\frac{1}{\alpha^i} - \mathrm{e}^{-\alpha l}\sum_{j=0}^{i}\frac{l^j}{j!\alpha^{i-j}}\right\} \tag{29b}$$

achieves the integration.

To calculate the $C(\mathbf{m})$ one has to perform the $l \to \infty$ limit on those $f(l;\mathbf{m})$ for which $|M(\mathbf{m})| = 0$. Note that for $|M(\mathbf{m})| = 0$ one always has $\alpha > 0$ since $\alpha = |M(\mathbf{m})| - |M(\mathbf{m}_1)| - |M(\mathbf{m}_2)| = 0$ and $|M(\mathbf{m})| = 0$ implies the vanishing of $|M(\mathbf{m}_1)|$ and of $|M(\mathbf{m}_2)|$. Hence the right hand side of equation (22) vanishes due to the square bracket containing the sign functions. So no such $f(l;\mathbf{m})$ is generated. Thus the $C(\mathbf{m})$ can be calculated by equation (29b) omitting the term proportional to $\mathrm{e}^{-\alpha l}$ on the right hand side.

The symmetry relations (18) can be used as a check of the results. The $C(\mathbf{m})$ are saved in a file together with the corresponding $\mathbf{m}$ for later usage. They are given up to order $k = 6$ in Appendix B. We intend to provide them up to order $k = 10$ in electronic form on our homepages on appearance of this article (see footnote p. 222).

Unfortunately, equation (22) implies also a natural limitation of the computation. Because of its recursive nature, the $f(l; \mathbf{m})$ of all preceding orders have to be stored. They are needed to derive the $f(l; \mathbf{m})$ in the current order. This leads to an exponential memory increase. To calculate all $C(\mathbf{m})$ to order $k = 10$ inclusively, we used about 30,000,000 basic data elements (27) occupying about 1GB RAM. Because of the extensive memory use we employed a SUN Ultra Enterprise 10000 which the Regional Computing Center of the University of Cologne kindly placed at our disposal. The calculation took about 12 h.

Table 1. Action of the operators $\mathcal{T}_i$ as defined by equation (33).

	$4\mathcal{T}_0^a$	
$\|t^{0,\pm 1}, s\rangle$	$\longrightarrow$	$-\|s, t^{0,\pm 1}\rangle$
	$4\mathcal{T}_0^b$	
$\|t^0, t^{\pm 1}\rangle$	$\longrightarrow$	$\|t^{\pm 1}, t^0\rangle$
$\|t^{\pm 1}, t^{\pm 1}\rangle$	$\longrightarrow$	$\|t^{\pm 1}, t^{\pm 1}\rangle$
$\|t^{\pm 1}, t^{\mp 1}\rangle$	$\longrightarrow$	$\|t^0, t^0\rangle - \|t^{\pm 1}, t^{\mp 1}\rangle$
$\|t^0, t^0\rangle$	$\longrightarrow$	$\|t^1, t^{-1}\rangle + \|t^{-1}, t^1\rangle$
	$4\mathcal{T}_1$	
$\|s, t^1\rangle, \|t^1, s\rangle$	$\longrightarrow$	$\|t^1, t^0\rangle - \|t^0, t^1\rangle$
$\|s, t^0\rangle, \|t^0, s\rangle$	$\longrightarrow$	$\|t^1, t^{-1}\rangle - \|t^{-1}, t^1\rangle$
$\|s, t^{-1}\rangle, \|t^{-1}, s\rangle$	$\longrightarrow$	$\|t^0, t^{-1}\rangle - \|t^{-1}, t^0\rangle$
	$4\mathcal{T}_2$	
$\|s, s\rangle$	$\longrightarrow$	$\|t^1, t^{-1}\rangle - \|t^0, t^0\rangle + \|t^{-1}, t^1\rangle$

3 Application: dimerized and frustrated S = 1/2 chain

In this section we demonstrate how the knowledge of the $C(\mathbf{m})$ in the effective Hamiltonian H_{eff} (25) permits to perform specific calculations. The first step is to evaluate the operators T_n for the model under study, here dimerized spin chains. Then we calculate the ground state energy, the energy gap and the one-magnon dispersion of the one-dimensional Heisenberg antiferromagnetic $S = \frac{1}{2}$ chain. This is again done by implementing the equations on a computer.

3.1 General equations

The explicit form of the operators T_n has to be determined so that

$$H_{\text{S}} = T_{-2} + T_{-1} + T_0 + T_1 + T_2 \tag{30}$$

(*cf.* Eqs. (2, 6b)). Let us consider one addend of H_{S} as starting point

$$\mathbf{S}_{2i}\mathbf{S}_{2i-1} + \alpha\left(\mathbf{S}_{2i}\mathbf{S}_{2i-2} + \mathbf{S}_{2i-1}\mathbf{S}_{2i+1}\right). \tag{31}$$

Obviously, only neighbouring dimers are affected. For simplicity we first calculate the matrix elements

$$\langle x_{i-1}, x_i|\mathbf{S}_{2i}\mathbf{S}_{2i-1}|x_{i-1}, x_i\rangle \tag{32}$$

where $x_{i-1}, x_i \in \{s, t^1, t^0, t^{-1}\}$ are singlets or one of the triplets on the adjacent dimers $i-1$ and i. The superscript $n \in \{0, \pm 1\}$ in t^n stands for the S^z component. For some fixed value of i we write

$$\mathbf{S}_{2i}\mathbf{S}_{2i-1} = \mathcal{T}_{-2} + \mathcal{T}_{-1} + \mathcal{T}_0 + \mathcal{T}_1 + \mathcal{T}_2 \tag{33}$$

requiring that the subscript indicates the net change of the number of triplets. In other words matrix elements connecting a ket of two singlets with a bra of two triplets belong to $\mathcal{T}_2$ and those connecting a ket of one singlet and one triplet with a bra of two triplets belong to $\mathcal{T}_1$ and so on. In this way one finds all the $\mathcal{T}_n$ and their sum is $\mathbf{S}_{2i}\mathbf{S}_{2i-1}$. Table 1 summarizes the results. For later convenience we split $\mathcal{T}_0 = \mathcal{T}_0^a + \mathcal{T}_0^b$. All other matrix elements can be constructed by using the relation $\mathcal{T}_n^\dagger = \mathcal{T}_{-n}$. To incorporate the effect of frustration it is sufficient to note that a triplet is invariant under spin exchange whereas a singlet acquires a factor -1. Let

$$\alpha(\mathbf{S}_{2i}\mathbf{S}_{2i-2} + \mathbf{S}_{2i-1}\mathbf{S}_{2i+1}) = \sum_{n=-2}^{2} \mathcal{T}'_n. \tag{34}$$

By spin exchange the $\mathcal{T}'_n$ operators defined in equation (34) are reduced to the $\mathcal{T}_i$ as given in Table 1

$$\mathcal{T}'_{\pm 2} = -2\alpha\mathcal{T}_{\pm 2} \tag{35a}$$

$$\mathcal{T}'_{\pm 1} = 0 \tag{35b}$$

$$\mathcal{T}_0^{'a} = -2\alpha\mathcal{T}_0^a \tag{35c}$$

$$\mathcal{T}_0^{'b} = 2\alpha\mathcal{T}_0^b. \tag{35d}$$

Finally, equation (30) implies

$$T_{\pm 2} = \sum_{i=0}^{\frac{L}{2}-1} (1 - 2\alpha)\mathcal{T}_{\pm 2} \tag{36a}$$

$$T_{\pm 1} = \sum_{i=0}^{\frac{L}{2}-1} \mathcal{T}_{\pm 1} \tag{36b}$$

$$T_0 = \sum_{i=0}^{\frac{L}{2}-1} (1 - 2\alpha)\mathcal{T}_0^a + (1 + 2\alpha)\mathcal{T}_0^b. \tag{36c}$$

The subsequent subsection shows how the T_n operators can be implemented.

For the antiferromagnetic $S = 1/2$ Heisenberg chain given by Hamiltonian (6) we can then calculate the ground state energy by

$$E_0 = \langle 0|H_{\text{eff}}|0\rangle \tag{37}$$

where we used the shorthand $|0\rangle := |\prod_i s_i\rangle$ for the product state of singlets on all dimers which can be viewed as triplet vacuum.

The actual calculations are done on finite clusters. From the linked cluster theorem we know that the finite order contribution of a short-ranged perturbation does not depend on the cluster size for sufficiently large clusters. In our one dimensional example only neighbouring dimers are linked. So it is sufficient to consider 11 dimers to avoid a wrap-around in order 10, *i.e.* for 11 dimers or more we are sure to find the thermodynamic contribution. Moreover, we can check the size-independence explicitly.

To calculate the one magnon dispersion we have to consider the subspace with exactly one single singlet being excited to a triplet. Using $|j\rangle = |s, s, \ldots, t, \ldots, s\rangle$ with one triplet t (S^z component does not matter) on dimer j we compute the action of the effective Hamiltonian (25) on $|j\rangle$. Since the number of triplets is conserved by construction the initial triplet can only be shifted.

$$H_{\text{eff}}|j\rangle = J\sum_i a_i|j+i\rangle. \tag{38}$$

The fact that the coefficients a_i do not depend on j relies on the translational invariance. All dimers are equal. But this is *not* necessary for our perturbation scheme to hold. On the contrary, we consider it one of the major advantages of the scheme presented here that it can be done in real space without knowing the form of the eigen states in advance.

In 10th order the variable i in equation (38) runs from -10 to 10. If j is chosen appropriately, a chain segment with 11 dimers suffices to compute all the coefficients a_i. For instance, for a_{10} one has to take $j = 0$ whereas for a_0 the right choice is $j = 5$. All sites that can be reached within 10 hops starting at j and ending at $j + i$ must be contained in the cluster to avoid finite size effects.

Of course, given translational invariance we know that spatial Fourier transform provides the eigen states $|k\rangle = \sqrt{2/L}\sum_i \exp(ikj)|j\rangle$ characterized by their lattice momentum k. The corresponding eigen energies read

$$\omega(k) = \langle k|\, H_{\text{eff}}\,|k\rangle - E_0 \tag{39a}$$

$$= Ja_0 - E_0 + J\sum_{j=1}^{\infty} 2a_j\cos(jk). \tag{39b}$$

For dimerized chains the dispersion minimum, the triplet gap, is found at $k = 0$

$$\Delta = \omega(k=0). \tag{40}$$

It is beyond the scope of the present paper to compute the effective Hamiltonian in the two-triplet sector. But an outlook on this issue is in order. Conventional perturbation schemes have difficulties to compute properties for two elementary particles because the structure of the eigen states is not known beforehand. In particular, bound states of two elementary particles are extremely difficult to obtain by conventional perturbative methods. But if the action of the effective Hamiltonian (25) on two triplets is calculated everything else can be deduced. First, one has to determine the coefficients $A_{i_1,i_2;j_1,j_2}$ defined by

$$H_{\text{eff}}|j_1, j_2\rangle = \sum_{i_i,i_2} A_{i_1,i_2;j_1,j_2}|i_1, i_2\rangle, \tag{41}$$

where we assume that $|j_1, j_2\rangle$ has a triplet t^1 on dimer j_1 and a triplet t^{-1} on dimer j_2. This is sufficient to compute triplets coupled to $S_{\text{tot}} = 1$ as was done successfully in reference [7]; the wave function $\psi(j_1, j_2)$ is antisymmetric under exchange $j_1 \leftrightarrow j_2$. Second, one has to diagonalize the matrix defined by the coefficients $A_{i_1,i_2;j_1,j_2}$. This can be carried out by standard Lanzcos algorithms.

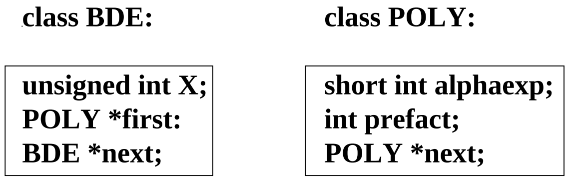

```
unsigned int X;
POLY *first:
BDE *next;
```

```
short int alphaexp;
int prefact;
POLY *next;
```

Fig. 1. Sketch of the basic data element class.

Spectral functions are also accessible by flow equation perturbation if the observable Q under study is unitarily transformed by the same transformation as the Hamiltonian

$$\frac{\mathrm{d}Q(\ell)}{\mathrm{d}\ell} = [\eta(\ell), Q(\ell)]. \tag{42}$$

This is needed to know the matrix elements after the transformation. Preliminary studies showed that the treatment of equation (42) is feasible within the perturbative approach. The necessary programmes are very similar to those for the Hamiltonian. Yet the treatment of observables is more laborious than the one of the Hamiltonian itself.

3.2 Computer aided evaluation

Again C++ is the programming language of our choice. To encode the states of the dimerized chain it suffices to reserve two bits per dimer. For instance, four bytes can encode the state of a chain with 32 sites. The lowest bit represents site 1, the second lowest represents site 2 and so on. By applying the T_i in equations (36) these states acquire polynomials in α as prefactors. Thus we choose the basic data elements to be objects of the class BDE as sketched in Figure 1.

The innermost part of the algorithm is the implementation of the $\mathcal{T}_i$ matrices. Each matrix element is represented by a block of C++ code. These blocks allocate an appropriate number of basic data elements initialized by the current state of the chain. Then they modify those bits which represent the pair of adjacent dimers under study according to the rules of Table 1. The T_i are implemented

$$
\begin{aligned}
\frac{\epsilon_0}{J} = (1-2\alpha)^2 \Bigg(& -\frac{3}{4}\overline{\lambda}^2 - \left(\frac{3}{4}+\frac{3}{2}\alpha\right)\overline{\lambda}^3 - \left(\frac{13}{16}+\frac{27}{4}\alpha-\frac{3}{4}\alpha^2\right)\overline{\lambda}^4 - \left(\frac{89}{48}+\frac{311}{24}\alpha+\frac{93}{4}\alpha^2-\frac{45}{2}\alpha^3\right)\overline{\lambda}^5 - \Bigg(\frac{463}{96}+\frac{227}{9}\alpha \\
& + \frac{1\,307}{12}\alpha^2 - 42\alpha^3 - \frac{159}{2}\alpha^4\Bigg)\overline{\lambda}^6 - \left(\frac{81\,557}{6\,912}+\frac{257\,909}{3\,456}\alpha+\frac{215\,995}{864}\alpha^2+\frac{173\,579}{432}\alpha^3-\frac{14\,865}{16}\alpha^4+\frac{879}{8}\alpha^5\right)\overline{\lambda}^7 - \Bigg(\frac{414\,359}{12\,960} \\
& + \frac{139\,801}{648}\alpha + \frac{8\,477\,587}{12\,960}\alpha^2 + \frac{152\,558}{81}\alpha^3 - \frac{2\,774\,357}{1\,620}\alpha^4 - 4\,002\alpha^5 + \frac{4\,527}{2}\alpha^6\Bigg)\overline{\lambda}^8 - \Bigg(\frac{2\,354\,594\,813}{24\,883\,200} + \frac{7\,341\,879\,263}{12\,441\,600}\alpha \\
& + \frac{14\,053\,262\,981}{6\,220\,800}\alpha^2 + \frac{1\,591\,335\,559}{345\,600}\alpha^3 + \frac{9\,560\,574\,943}{1\,555\,200}\alpha^4 - \frac{8\,121\,212\,969}{259\,200}\alpha^5 + \frac{453\,741}{64}\alpha^6 + \frac{248\,391}{32}\alpha^7\Bigg)\overline{\lambda}^9 \\
& - \Bigg(\frac{106\,469\,295\,871}{373\,248\,000} + \frac{8\,284\,9717\,337}{46\,656\,000}\alpha + \frac{107\,584\,683\,283}{15\,552\,000}\alpha^2 + \frac{89\,796\,462\,557}{5\,832\,000}\alpha^3 + \frac{160\,938\,279\,937}{5\,832\,000}\alpha^4 - \frac{57\,686\,123\,141}{972\,000}\alpha^5 \\
& - \frac{143\,920\,286\,959}{972\,000}\alpha^6 + \frac{339\,171}{2}\alpha^7 - \frac{336\,527}{16}\alpha^8\Bigg)\overline{\lambda}^{10}\Bigg),
\end{aligned}
\tag{44}
$$

---

in five steps:

(i) The number of sites L is chosen even. We introduce the loop variable

$$p \in \left\{1, 2, \ldots, \frac{L}{2}\right\} \tag{43}$$

such that $p = 1$ addresses dimer 0 together with dimer 1, $p = 2$ addresses dimer 2 and dimer 1 and so on. Periodic boundary conditions are used, *i.e.* $p = L/2$ addresses dimer $L/2 - 1$ with dimer 0.

(ii) From p a four byte long bit mask is constructed such that the bits referring to the dimers addressed by p are set to unity and zero otherwise. Thus $p = 1$ yields $(1, 1, 1, 1, 0, \ldots, 0)$ and $p = 2$ yields $(0, 0, 1, 1, 1, 1, 0, \ldots, 0)$ and so on .

(iii) The appropriate part x representing the two adjacent dimers is cut out by applying the logical AND operation: (bit mask) AND (X representing the chain state).

(iv) The decimal value of $x \in \{0, 1, \ldots, 15\}$ is used to jump in a SWITCH(x)-CASE sequence to the appropriate CASE-block, encoding the matrix element of $\mathcal{T}_i$.

(v) The appropriate prefactor is multiplied to the allocated and modified data elements.

Finally p is incremented by one and one goes back to (i) as long as p meets condition (43).

Following these steps one obtains a sum of basic data elements describing an elementary chain state after the application of a T_i. In general, the complete state after the application of a T_i is a linear combination of such elementary states encoded by the unsigned integers X. The linear combination is stored as a list. Since this list after its generation may contain identical states it is sorted according to increasing values of X by a quick-sort algorithm. Prefactors of identical states are added so that memory usage is reduced.

To calculate products of T_i, the algorithm described above is applied repeatedly. If the chain state is a linear combination the algorithm is applied to each addend of this linear combination.

To calculate the ground state energy (37) the expression $\lambda^k \sum_{|\mathbf{m}|=k} C(\mathbf{m})T(\mathbf{m})$ from equation (25) must be applied to the triplet vacuum $|0\rangle$ for each order k. First the current index $\mathbf{m}$ and its coefficient $C(\mathbf{m})$ are read from an input file prepared previously, see Section 2.2. Then $T(\mathbf{m})$ is applied to $|0\rangle$ as described above. Since $M(\mathbf{m}) = 0$, $T(\mathbf{m})$ reproduces $|0\rangle$ up to a prefactor which is a polynomial in α. This polynomial and $C(\mathbf{m})$ are piped to an algebraic computer programme (Maple) to multiply them. This scheme is iterated with intermediate summations by Maple till the final result is found.

The result for the ground state energy per spin of the Hamiltonian (6) up to 10th order in λ reads

see equation (44) above

where the shorthand $\overline{\lambda} = \frac{1}{4}\lambda$ is used.

To calculate the dispersion $\omega(k)$ the hopping elements a_i in equation (39b) have to be determined. The effect of $T(\mathbf{m})$ with $M(\mathbf{m}) = 0$ is to shift a triplet by at most $|\mathbf{m}|$ dimers. Hence it suffices to perform the calculation for a given a_i on an appropriate chain segment. The calculations are analogous to those for the ground state energy. Note that by equation (38) the general effect of a product $T(\mathbf{m})$ will be a sum of states each containing one triplet on different dimers. For a given a_i the corresponding state has to be found in that list. Its polynomial prefactor yields a_i. Results for the hopping elements up to 6th order in λ are presented in Appendix C.

The calculations took 10 h–30 h strongly depending on the number of sites L; 100MB-500MB memory were used. The computations were done on a Sun Ultra workstation.

4 Results and comparison to other methods

So far all results refer to Hamiltonian (4). In this section we prefer to present the results corresponding to Hamiltonian (3) by substituting according to equation (5). Since λ is the expansion parameter it is substituted *before* we manipulate the equations further, see below. The frustration α on the other hand is treated as a fixed parameter throughout further manipulations. It is substituted only at the very end.

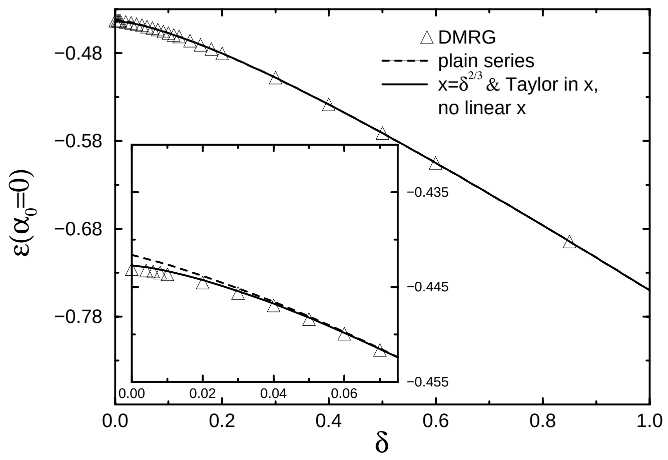

Fig. 2. Ground state energy per site ϵ *vs.* dimerization δ without frustration ($\alpha_0 = 0$) for Hamiltonian (4). For details see main text. The inset shows an enlargement for small δ.

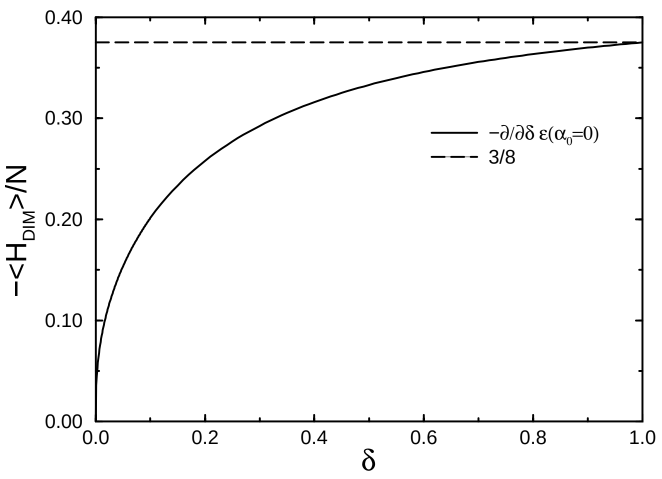

Fig. 3. Expectation value of the dimerization operator H_{DIM} *vs.* dimerization δ without frustration ($\alpha_0 = 0$).

4.1 Ground state energy

Substituting J, λ and α in equation (44) leads to the dashed curve in Figure 2 called "plain series". The solid line represents a more sophisticated approach. Substituting J and λ leads to an expression in δ and α. In order to profit from the knowledge that the ground state energy is lowered by external dimerization as $\Delta E_0 \propto -\delta^{4/3}$ [15] $\delta = x^{3/2}$ is substituted. Thereby α is treated as fixed parameter which does not change the exponents, here 4/3. Their values are protected by symmetry [16] as long as logarithmic corrections are neglected [17,18]. This means that this statement is true as long as α is below its critical value $\alpha_{\mathrm{c}} = 0.241167(\pm 5)$ [19]. Above this value the translational invariance is broken spontaneously and the ground state is dimerized so that the leading power becomes linear $\Delta E_0 \propto -\delta$ (see below).

The result for the ground state energy is expanded in a Taylor series in x up to order 10 about $x = 1$. This is the limit of strong dimerization for which our expansion holds. Adding the term $Y(1-x)^{11}$ introduces an unknown Y which can be fitted such that the linear term in x vanishes. In this way the leading order contribution to the energy lowering agrees with the continuum prediction. The result of this procedure is depicted as solid curve in Figure 2 and is labeled accordingly. Both curves are compared to numeric results from Density Matrix Renormalization Group (DMRG) shown as symbols. The agreement is excellent. The accordance is better for the biased extrapolation based on the continuum theoretical power law as was to be expected. The extrapolated results can be trusted even quantitatively down to 1 or 2% dimerization.

In absence of frustration ($\alpha = \alpha_0 = 0$) the right hand side of equation (44) becomes a polynomial in λ of degree 10 with rational coefficients. Using a different perturbation method Barnes *et al.* [20] calculated the same coefficients up to order 9, providing a good check. Furthermore, Gelfand *et al.* [21] also calculated a polynomial in λ. Their method gives the coefficients as real numbers up to order 15. We could verify these numbers to the given precision in reference [21] up to order 10.

One of the major motivations to study dimerized spin chains comes from spin-Peierls systems where spin and lattice degrees of freedom are coupled. In the adiabatic description of this phenomenon one adds the elastic energy $\frac{K}{2}\delta^2$ to the Hamiltonian (3). This term takes into account that it costs energy to modulate the magnetic couplings. To determine the equilibrium value of δ the ground state energy is minimized by variation of δ

$$0 = \frac{\partial \epsilon_0}{\partial \delta} + K\delta. \tag{45}$$

So one has to know the derivative of ϵ_0 which is given by the expectation value per site of the dimerization operator $H_{\mathrm{DIM}} = (H(\delta) - H(0))/\delta$ with H from equation (3)

$$\frac{\langle H_{\mathrm{DIM}} \rangle}{L} = \frac{\partial \epsilon_0}{\partial \delta}\,. \tag{46}$$

In Figure 3 we plot $\partial\epsilon_0/\partial\delta$ as derived from our results for the ground state energy. Note that 3/8 is an upper bound for the expectation value of the dimerization since the dimerization is maximum if every second bond is occupied by a singlet $\langle \mathbf{S}_{2j}\mathbf{S}_{2j+1}\rangle = -3/4$. This upper bound is excellently complied with by our results since we expand around the limit of complete dimerization $\delta = 1$.

Figure 4 shows the ground state energy per site for $\alpha_0 = 0.241$ and $\alpha_0 = 0.35$. For supercritical frustration we know that the leading term is linear in δ. In order to be able to describe well the crossover from $\delta^{4/3}$ to δ behavior we use the substitution $\delta = x^3$ and suppress linear and quadratic terms in the Taylor expansion by appropriate higher order terms in $(1-x)$. This procedure leads to a series in δ comprising terms $\propto \delta$ and $\propto \delta^{4/3}$ as well as higher terms in $\delta^{1/3}$. The agreement obtained in comparison to DMRG data is again excellent down to very low values of dimerization. In Figure 5 the expectation values of the corresponding dimerization operators H_{DIM} are plotted.

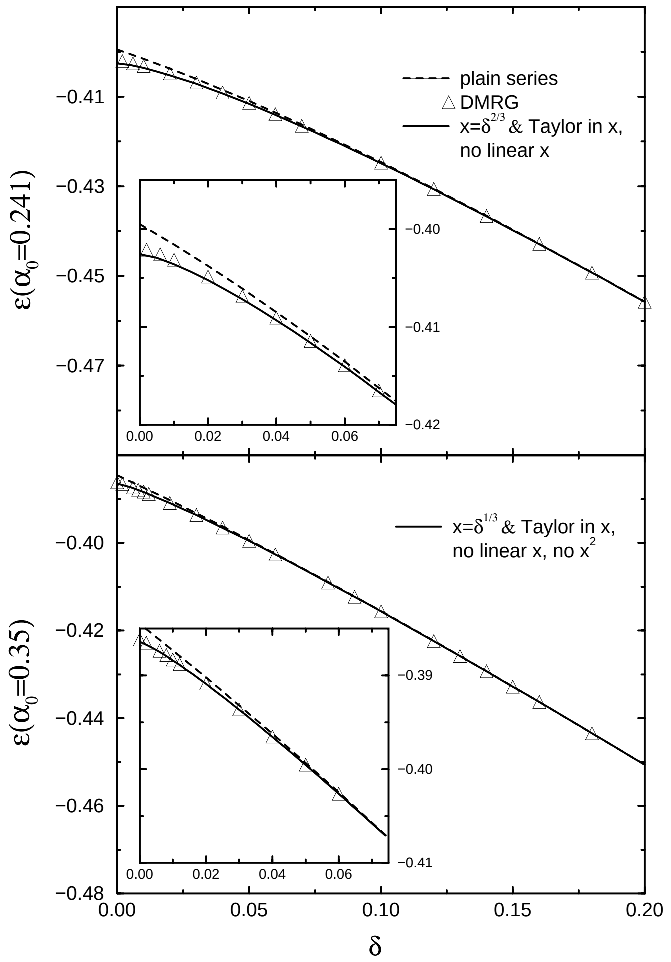

Fig. 4. Ground state energy ϵ *vs.* dimerization δ; frustration $\alpha_0 = 0.241$ (upper panel), $\alpha_0 = 0.35$ (lower panel). The insets show enlargements for small δ.

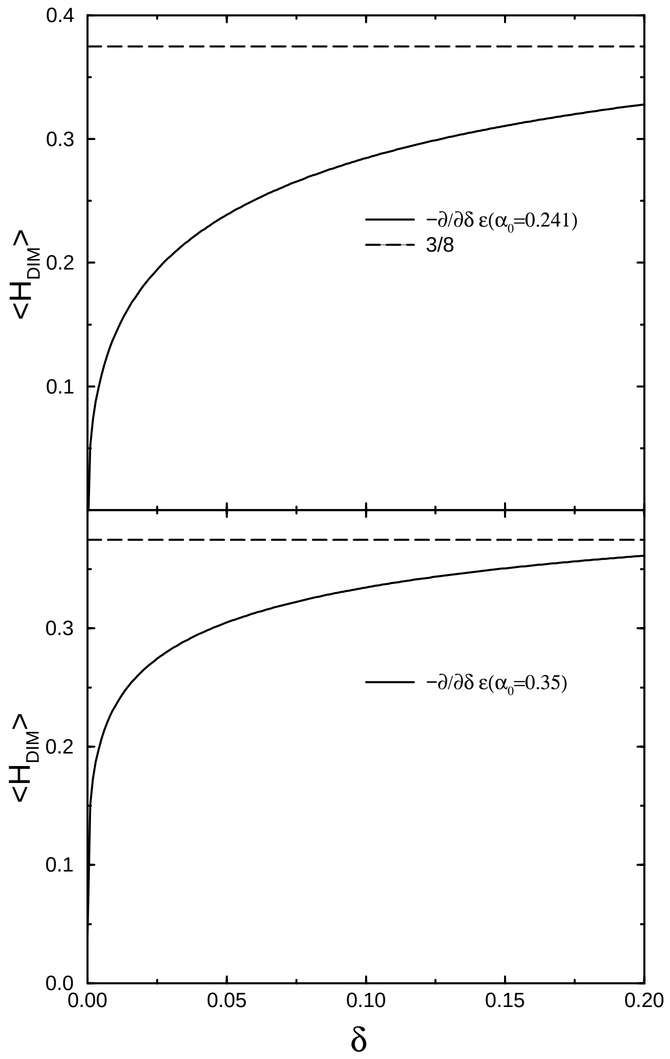

Fig. 5. Expectation value of the dimerization operator $H_{\rm DIM}$ *vs.* dimerization δ; frustration $\alpha_0 = 0.241$ (upper panel), $\alpha_0 = 0.35$ (lower panel).

We limited the range of δ for finite frustration to the interval $[0, 0.2]$. This is required by the nature of our perturbative expansion around isolated dimers. Fixing α_0 (not α!) at a finite value implies that the limit $\delta \to 1$ is *not* the limit of isolated dimers. The point $\delta = 1$ corresponds to a spin ladder with coupling $2J_0$ on the rungs and $\alpha_0 J_0$ on the legs. Of course, our bare perturbative results pertain also to the ladder where they correspond to an expansion around the rung limit. This limit has already been investigated intensively [22] so that we refrain here from a comprehensive analysis. Note that the perturbation in the ladder is considerably simpler since $N = 1$ in equation (2) whereas $N = 2$ is treated here. In other words there is no creation or annihilation of *two* triplets but only shifts of triplets or creation or annihilation of one triplet.

To understand the reason for the restricted applicability of the analysis presented here a simple comparison of couplings suffices. Using $x = \delta^{2/3}$ or $x = \delta^{1/3}$ is optimized to treat the case where the coupling $J_0(1-\delta)$ is the dominant perturbation. As a rule of thumb this is the case if $2\alpha_0 < 1 - \delta$. Otherwise one has to treat the frustrating coupling as the dominant perturbation. We restrict our present analysis to the regime where the $1 - \delta$ coupling is the dominant perturbation so that δ may not be chosen too large. For $\alpha_0 \approx 0.35$ the dimerization δ should not exceed about 0.3.

4.2 Energy gap

The first approach is again to substitute J, λ and α in equation (40) according to equation (5). In the case $\alpha_0 = 0$ our result agrees to the 9th degree polynomial Barnes *et al.* [20] computed for the energy gap. For various values of α_0 the results are plotted as dashed curves labeled “plain series” in Figures 6, 7 and 8.

The solid curves were obtained by an extrapolation biased by the continuum theory results $\varDelta \propto \delta^{2/3}$ for subcritical frustration [15] and $\varDelta - \varDelta|_{\delta=0} \propto \delta^{2/3}$ for supercritical frustration, see *e.g.* reference [23]. To this end, we substituted J and λ in equation (40) according to equation (5).

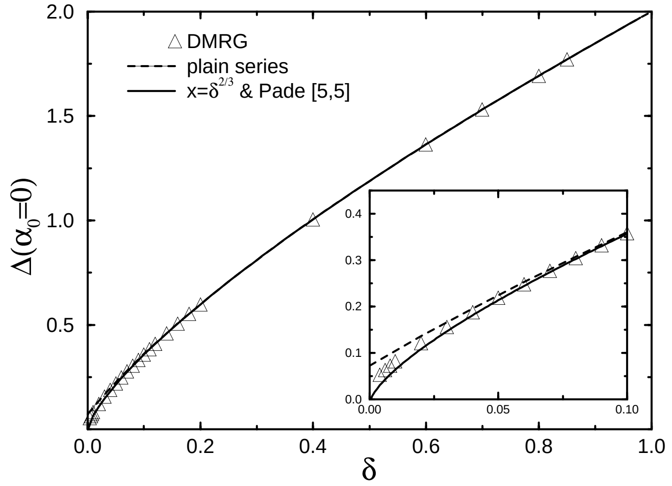

Fig. 6. Energy gap Δ *vs.* dimerization δ without frustration. The numbers in the square bracket stand for the polynomial degree in the numerator and the denominator of the Padé approximant, respectively. The inset shows an enlargement for small δ.

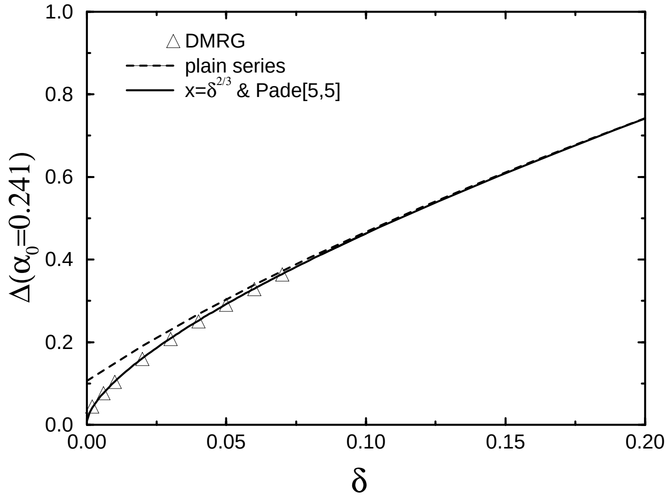

Fig. 7. Energy gap Δ *vs.* dimerization δ for critical frustration $\alpha_0 = 0.241$.

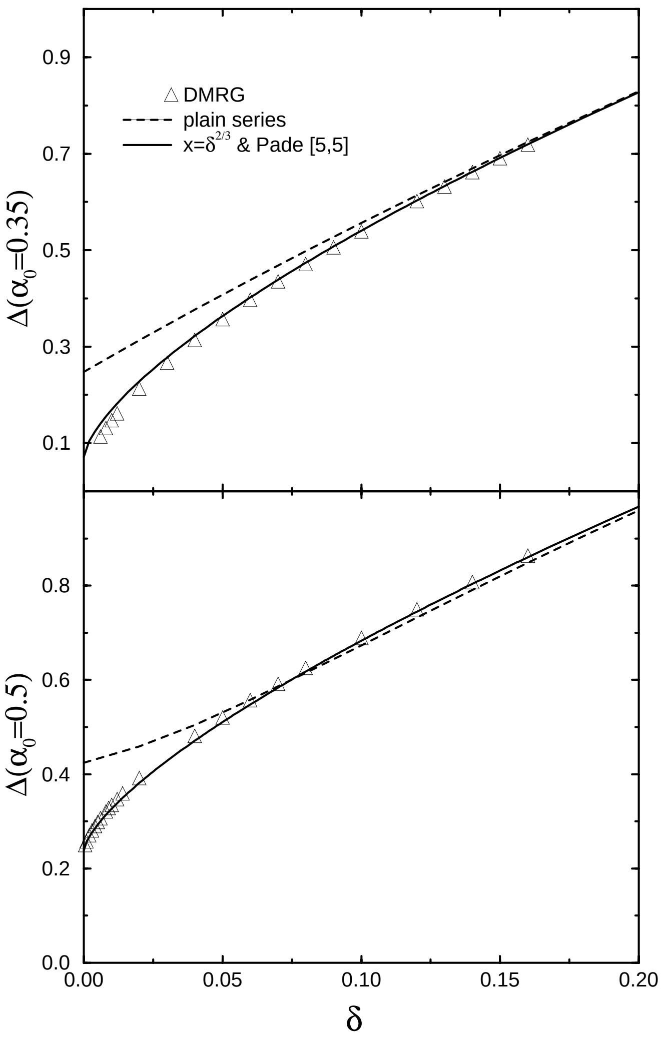

Fig. 8. Energy gap Δ *vs.* dimerization δ for supercritical frustration $\alpha_0 = 0.35$, $\alpha_0 = 0.5$.

Next $\delta = x^{3/2}$ is replaced treating α as a fixed parameter. This result is re-expressed by an appropriate Padé approximant about $x = 1$, which corresponds to the dimer limit. As will be seen below the use of a Padé approximant instead of a series in x matters only for sizable frustration. The Padé approximant is chosen such that it takes the information about the 11 coefficients of the expansion into account. In the final expression $x = \delta^{3/2}$ and $\alpha = \frac{\alpha_0}{1-\delta}$ are inserted to obtain the data shown. The comparison to DMRG data [23] shows that the biased extrapolation is extremely precise for most choices of parameters.

In order to check the reliability of our results in the most difficult case we extrapolate our results to zero dimerization. This means we employ the above procedure of a biased Padé approximant and set $\delta = 0$. The gap dependence on the frustration α_0 is depicted in Figure 9 and compared to DMRG results [24,25]. For comparison we include also an extrapolation of the series in $x = \delta^{2/3}$. Rigorously, there is no gap below the critical value α_c [26]. The numerical value ($\alpha_c = 0.241167(\pm 5)$) is taken from reference [19]. The wiggle at about $\delta = 0.1$ is a spurious pole resulting from the Padé approximation which is not present in the series representation. The Padé approximant, however, is better for larger frustration. The overall agreement is good but not excellent. Obviously, neither the Padé approximant nor the series in x are fit to describe the essential singularity at critical frustration. Yet, more sophisticated approximants which allow to extrapolated in several variables (here: λ and α_0) might render a more efficient analysis of the available expansion coefficients.

To complete the analysis of our expansion coefficients other approximants were also used. The common approach to detect critical behaviour is to approximate the derived logarithm of the function under study by a Padé approximant (Dlog Padé). In this representation the position

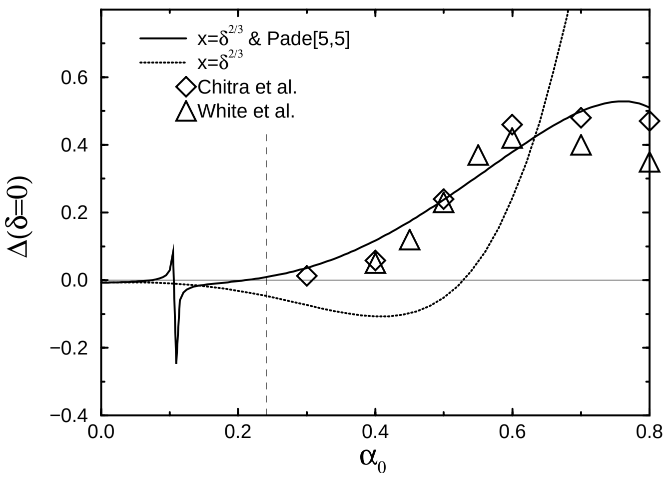

Fig. 9. Energy gap Δ *vs.* frustration α at $\delta = 0$. The dashed vertical line indicates the value of α_c.

λ_c of a singularity $(\lambda - \lambda_c)^\gamma$ is given by a pole and its residue defines the critical exponent γ. The results do not depend much on whether the Hamiltonian (3) or (4) is used. In fact, the results for Hamiltonian (4) agree a bit better with the predictions $\lambda_c = 1$ and $\gamma = 2/3$ than those for Hamiltonian (3). In absence of frustration we find $\lambda_c = 1.002$ and $\gamma = 0.74$. The value for the position is very encouraging; the result for the critical exponent, however, is a bit disappointing. The same observation was made in reference [20]. No significant change in the exponent occurs if the position of the singularity $\lambda_c = 1$ is pre-set.

The reason for the difficulty to find the correct exponent is found in the logarithmic corrections. This can be seen in two ways. The first one is to go to the critical frustration where no logarithmic corrections are present. This proved useful in numerical analyses [24], too. Indeed, at $\alpha_0 = \alpha_c$ we find $\gamma = 0.65$ which agrees with 2/3 within 3%. The second is to take the logarithmic corrections into account. Usually, they are computed for subcritical frustration and given in the form [27,17,18]

$$\Delta(\delta) \propto \delta^{2/3}/|\ln(\delta/\delta_0)|^{1/2} \tag{47}$$

where δ_0 is some unknown constant. Hence, we apply the Dlog Padé approximation to

$$f(\delta) := \sqrt{-\ln(\delta) + h(\alpha_0)}\,\Delta, \tag{48}$$

where $h(\alpha_0)$ is some constant depending on the frustration. We look at the biased approximant $f'/f = P(\delta^2)/\delta$ about $\delta^2 = 1$ where $P(\delta^2)$ is a polynomial of order 9 in δ^2 which takes the obvious symmetry $\delta \leftrightarrow -\delta$ of Hamiltonian (3) into account. To be able to expand about isolated dimers the replacement $\alpha_0 \to \alpha_0(1 - \delta^2)$ is carried out. The value $P(0)$ then is a direct estimate for the critical exponent γ. Assuming that the coefficients of P decrease quickly on increasing order once the logarithmic correction is properly taken into account we fix the constant $h(\alpha_0)$ such that the coefficient of order 9 vanishes. In this way we find $\gamma = 0.68$ and $h = 5.65$ at zero frustration. At critical frustration the values are 0.56 and 2.50, respectively.

The good agreement without frustration indicates that logarithmic corrections are indeed the reason for the difficulty to determine the correct exponents from the perturbative data. The unsatisfactory agreement at critical frustration tells us that the way h is determined is not optimum. It would be very helpful if a prediction for the gap as function of δ and $\alpha - \alpha_c$ existed which comprised also the regime of supercritical frustration.

4.3 Dispersions

The one magnon dispersion $\omega(k)$ for the antiferromagnetic Heisenberg chain is given by equation (39b). The hopping elements a_i are given in Appendix C. For $\alpha_0 = 0$ they can be compared till order 5 with those computed in reference [20]. Full agreement is found.

To deduce the dispersion relations from the bare coefficients several approaches will be presented. The direct approach is again to substitute J, λ and α in equation (39b) according to equation (5). By construction, the resulting curves reproduce the same energy gaps at $k = 0$ as the gap results labeled "plain series" in the preceding section. We learned, however, in the preceding section that a biased extrapolation is very useful to approximate the gaps. So the question arises how the good biased extrapolations can be used for the description of dispersion relations.

Motivated by the behaviour of Lorentz-invariant systems where the dispersion passes from $\omega = v_S k$ (v_S spin wave velocity) to $\omega \propto \sqrt{\Delta^2 + (v_S k)^2}$ when a gap opens we use the following procedure. We substitute J and λ into equation (39b) leading to the plain series result we shall refer to as $\omega_{\text{plain}}(k;\alpha)$. Then the difference

$$\omega^2_{\text{diff}}(k) := \omega^2_{\text{plain}}(k;\alpha) - \omega^2_{\text{plain}}(k = 0;\alpha) \tag{49}$$

is expanded as Taylor series about $\delta = 1$ up to 10th order while α is treated as fixed parameter. Only then α is substituted according to equation (5). Finally, the dispersion is computed by the quadratic mean

$$\omega(k) = \sqrt{\Delta^2(\alpha_0, \delta) + \omega^2_{\text{diff}}(k)}. \tag{50}$$

For $\delta = \alpha_0 = 0$ the result is shown in Figure 10 where it is also compared to the plain series result to illustrate the effect of the quadratic mean. Both curves are compared to the rigorous result known from Bethe ansatz [28]. The quadratic mean matters only for low energies. Figures 11, 12 and 13 show the corresponding results for various δ and α values for relatively low frustration in the subcritical regime or close to it. As soon as there is some dimerization, for instance $\delta \geq 0.05$ in Figure 11, the difference between the plain series (not shown) and the quadratic mean (50) is no longer discernible.

Entering the regime of large frustration ($\alpha_0 > 0.4$) the calculations have to be modified slightly. In Figure 14 we compare two different approaches to calculate the dispersion $\omega(k)$. The dashed line labeled "$\omega_{\text{plain}}(k)$ & Taylor"

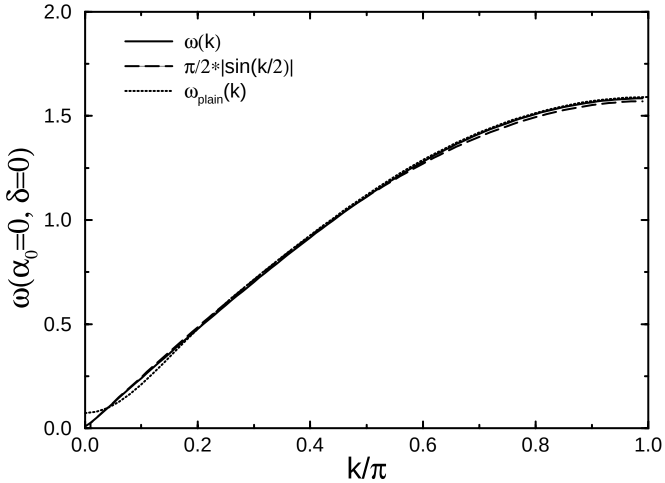

Fig. 10. Dispersion ω *vs.* wave vector k without frustration and dimerization.The curve ω_{plain} depicts the plain series result.

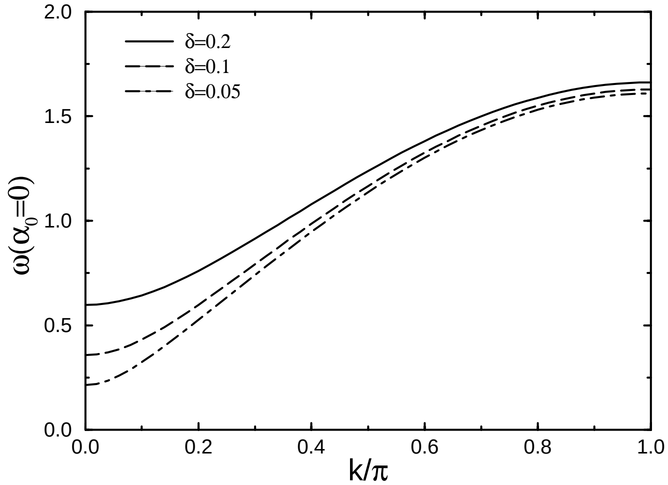

Fig. 11. Dispersion ω *vs.* wave vector k at $\alpha_0 = 0$ and various dimerizations.

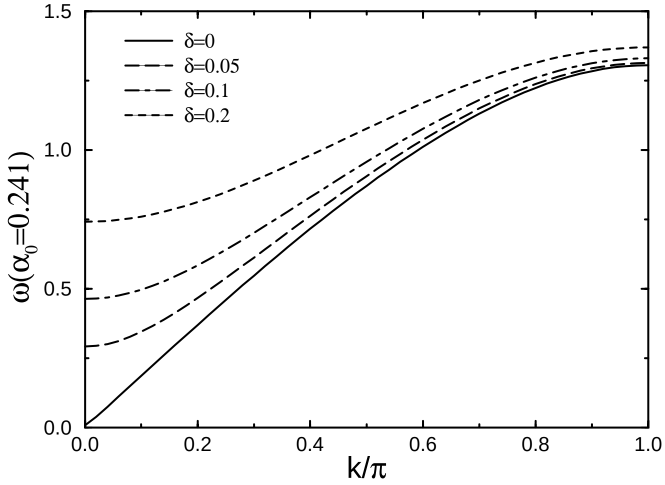

Fig. 12. Dispersion ω *vs.* wave vector k at $\alpha_0 = 0.241$ and various dimerizations.

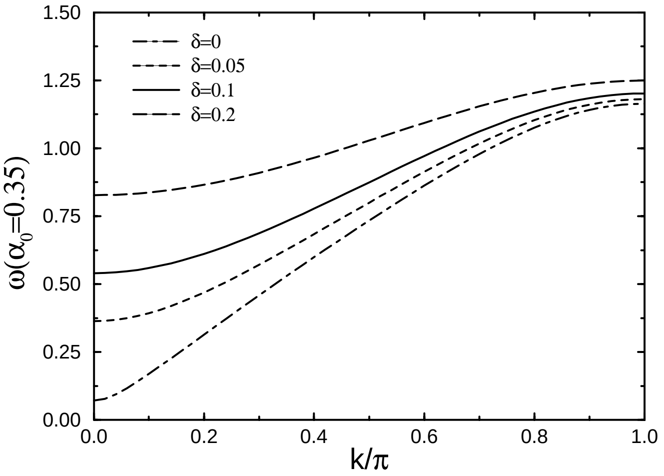

Fig. 13. Dispersion ω *vs.* wave vector k at $\alpha_0 = 0.35$ and various dimerizations.

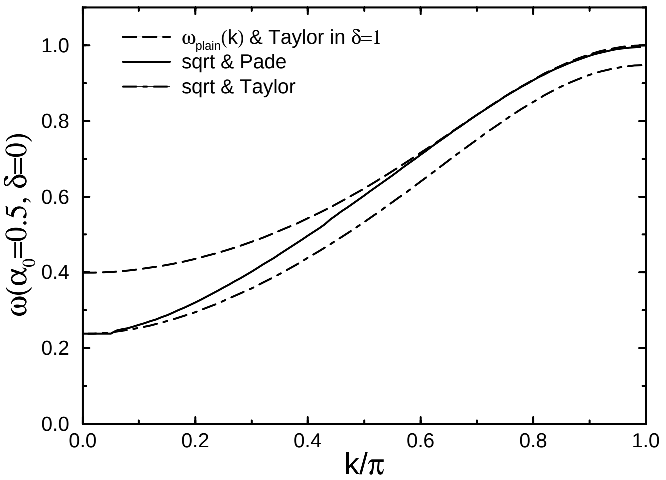

Fig. 14. Dispersion ω *vs.* wave vector k at $\alpha_0 = 0.5$ and $\delta = 0$. The results of three different ways to deduce the dispersion relation from the bare coefficients are depicted.

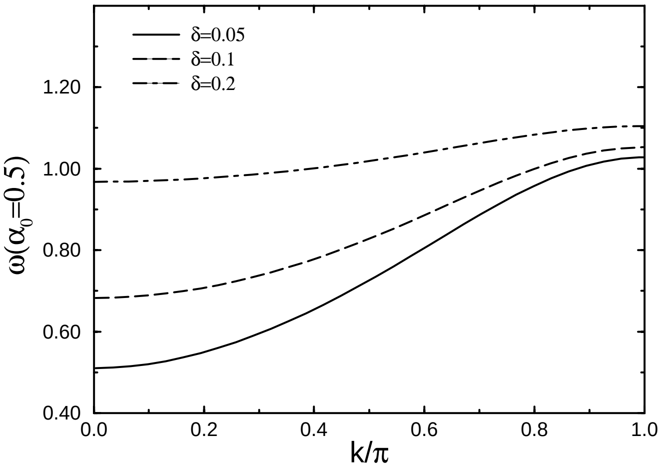

Fig. 15. Dispersion ω *vs.* wave vector k at $\alpha_0 = 0.5$ and various dimerizations. The approach used is the one labeled sqrt & Pade in Figure 14.

is obtained by expanding $\omega_{\text{plain}}(k;\alpha)$ in a Taylor series about $\delta = 1$ with α as fixed parameter. Finally, α is substituted according to equation (5) for $\delta = 0$, $\alpha_0 = 0.5$. The resulting curve is far off for low wave vectors. To get good values for the energy gap it is necessary to use the square root representation (50). On the other hand, the value at $k = \pi$ is unity which is the exact result [29,30]. If the square root representation (50) is used the dashed-dotted line labeled "sqrt & Taylor" in Figure 14 is obtained. The energy gap is nicely reproduced [30] but the agreement at the dispersion maximum deteriorates considerably.

So one would like to have a representation at hand which combines the advantages of the two approaches. A convincing interpolation is achieved by replacing the Taylor series by the corresponding [5,5] Padé approximant labeled "sqrt & Padé" in Figure 14. Figure 15 presents the results of the latter approach for finite δ. For completeness, we mention that in the $\alpha_0 \leq 0.4$ regime the Padé representation works as well as the Taylor expansion. For instance, the Padé representation reproduces the results presented in Figure 13 within 1%. This means that for $\alpha_0 \leq 0.4$ there is no need to use the more tedious Padé representation. But its use for larger frustrations does not imply an inconsistency of our general approach.

The observation that the dispersion relation for strong frustration behaves at $k \approx 0$ and at $k \approx \pi$ qualitatively differently can be understood on physical grounds. For this purpose let us consider the Majumdar-Ghosh model at $\alpha_0 = 1/2$ without dimerization. Its low-lying excitations are asymptotically free $S = 1/2$ spinons [31–33,30]. This implies that in the vicinity of the dispersion minimum the dispersion relation for $\delta \to 0$ does not represent the branch of a well-defined magnon excitation. But it is the lower band edge of a two-spinon continuum. In this respect it is similar to the situation of subcritical frustration. So we have to use the corresponding appropriate extrapolation to obtain reliable results.

In the vicinity of the dispersion maximum, however, the spinon interaction dominates over the kinetic energy and binding occurs even without dimerization. For instance, the exact triplet state [29] is a tightly bound two-spinon state. A variational analysis shows that this bound triplet exists below the two-spinon continuum in a finite interval around $k = \pi$ [31,33,30]. Hence, it is fully comprehensible that the perturbative approach which starts from local triplets works more easily around $k = \pi$ whereas improved extrapolation is necessary around $k = 0$.

5 Conclusions

In summary, we presented a perturbative scheme which relies on a suitably chosen unitary transformation. The scheme works for an unperturbed equidistant spectrum which can be labeled by the number of energy quanta. The perturbation term changes the number of energy quanta at maximum by a finite number N. Thereby, we generalized the approach by Stein ($N = 1$) [8] to general N. The unitary transformation is carried out by flow equations [10].

By the transformation a systematic mapping of the original problem to an effective Hamiltonian is achieved which conserves the number of energy quanta. Thus Hilbert space sectors with different number of energy quanta are separated. Our scheme will be particularly useful where ordinary perturbation theory is hampered by the fact that the structure of the perturbed states is not known, for instance, systems without translation invariance or two-particle problems. The possibility to obtain information in symbolic form, *i.e.* as polynomials, distinguishes our approach from the multiprecision method by Barnes *et al.* [20] and other conventional implementations [21].

The realization of the perturbative scheme comprises two distinct steps. The first is still general, the second specific to the model. For the first step we provided the necessary coefficient up to order 10 for $N = 2$. In written form they are included till order 6 in this publication. The other coefficients shall be provided electronically.

The second step is illustrated by dimerized frustrated $S = 1/2$ chains. The limit of isolated dimers has an equidistant spectrum. The ground state is the product of singlets on the dimers. The energy quanta are triplets on the dimers. The perturbing weak couplings between the dimers may create/annihilate at most two triplets so that $N = 2$ holds. After the transformation the number of triplets is conserved. We presented results for the ground state (zero triplets) and the magnon dispersion (one triplet). Thereby we demonstrated the validity and applicability of the scheme proposed.

The results for the spin chains are given as polynomials in λ and in the frustration parameter α. So they are easy to use for anybody who wants to analyze data by appropriate fits. No new calculations are necessary. The fits can be carried out instantly. Based on the results for the dimerization operator H_{D} the dependence of the dimerization δ on the elastic spring constant K is quickly accessible.

As we demonstrated our results are reliable down to about 6% *without* additional information, *i.e.* using the plain series. *With* additional information as the critical exponent, for instance, the results can reliably be used down to about 2%, in some cases even less. Moreover, starting from the exact coefficients more elaborate schemes like differential approximants in two variables become possible [34].

As an outlook we like to point out that our approach can also be used to compute dispersion relations in two or higher dimensional dimerized spin systems as demonstrated recently for $(\text{VO})_2\text{P}_2\text{O}_7$ [7]. Investigations for CuGeO_3 are in preparation. They will improve considerably the third order analysis [35]. Another fascinating field concerns computations in the two-magnon sector. The attractive interaction of two magnons [16], for instance, leads to bound states. For $(\text{VO})_2\text{P}_2\text{O}_7$, which is characterized by a relatively large dimerization, such results were found in a fourth order calculation. If the unitary transformation is applied to observables like, for instance, the Raman operator spectral functions are also within reach.

We acknowledge many fruitful discussions with E. Müller-Hartmann and F. Schönfeld. We are indebted to the latter also for the DMRG results which we used as a benchmark. This work was supported by the Deutsche Forschungsgemeinschaft in the SFB 341 and in the Schwerpunkt 1073. The large scale computations were done on machines of the Regional Computing Center of the University of Cologne.

Note added in proof

After acceptance of the manuscript we became aware of two related works using other expansion techniques around the dimer limit. These results are computed at fixed values of the frustration α_0 but partially at higher order (λ^{23} for the ground state energy, λ^{11} for the dispersion for $\alpha_0 \in \{0, 0.2411, 0.5\}$ in R.R.P. Singh and Z. Weihong, Phys. Rev. B **59**, 9911 (1999); λ^{10} for the gap at $\alpha_0 = 0$ in A. Honecker, Phys. Rev. B **59**, 6790 (1999)).

Appendix A: Proof of block diagonality

It is shown that the choice (12) for the infinitesimal generator achieves block diagonality for the effective Hamiltonian $H(\ell = \infty)$. The proof follows the lines of Mielkes proof for band matrices [14]. Let $\{|\nu_i\rangle\}$ be the eigen state basis of H_0 and define

$$\begin{aligned} h_{ij}(\ell) &:= \langle \nu_i | H(\ell) | \nu_j \rangle \\ h^0_{ij} &:= \langle \nu_i | H_0 | \nu_j \rangle \\ \eta_{ij}(\ell) &:= \langle \nu_i | \eta(\ell) | \nu_j \rangle. \end{aligned}$$

Inspecting equations (9, 10, 12) closely one realizes that the choice for the infinitesimal generator is equivalent to

$$\eta_{ij}(\ell) = \mathrm{sgn}(h^0_{ii} - h^0_{jj}) h_{ij}(\ell). \tag{A.1}$$

Inserting this expression in flow equation (8) yields

$$\begin{aligned} \frac{\partial h_{ij}}{\partial \ell} &= -\mathrm{sgn}(h^0_{ii} - h^0_{jj})(h_{ii} - h_{jj}) h_{ij} \\ &\quad + \sum_{k \neq i,j} (\mathrm{sgn}(h^0_{ii} - h^0_{kk}) + \mathrm{sgn}(h^0_{jj} - h^0_{kk})) |h_{ik}|^2. \end{aligned} \tag{A.2}$$

Assume without loss of generality that the eigen states $|\nu_i\rangle$ are labeled such that $h^0_{kk} \geq h^0_{ii}$ if $k > i$. Let us consider the sum of the first r diagonal elements of $H(\ell)$

$$\frac{\partial}{\partial \ell} \sum_{i=1}^{r} h_{ii} = 2 \sum_{i=1}^{r} \sum_{k > r} \mathrm{sgn}(h^0_{ii} - h^0_{kk}) |h_{ik}|^2. \tag{A.3}$$

The right side of equation (A.3) is non-positive. Thus the sum on the left hand side is a continuous monotonically decreasing function with ℓ. If we know that it is bounded from below we conclude that the sum converges whence the vanishing of its derivative for $\ell \to \infty$ ensues immediately. Hence we need beyond the conditions (i) and (ii) in the Introduction the boundedness for the whole Hamiltonian. If this is not given our choice for η might be problematic whereas Wegner's choice still works (for an example, see Ref. [36]).

As we are, however, interested in deriving a perturbation expansion order by order we can assume the whole Hamiltonian to be bounded from below without loss of generality. For any finite order of the expansion it is sufficient to consider a finite cluster supposing some short range interaction. Then the Hamiltonian is a finite dimensional matrix and is certainly bounded from below. This is true in particular if we stay on the abstract level as in equation (2). The generalized variational principle implies that

$$\sum_{i=1}^{r} h_{ii} \geq \sum_{i=1}^{r} \omega_i \tag{A.4}$$

holds for all ℓ where the ω_i are the eigen values of H in ascending order. Note that the eigen values are invariant under the unitary transformation.

The vanishing of the derivative of $\sum_{i=1}^{r} h_{ii}$ for arbitrary r implies eventually

$$\lim_{\ell \to \infty} \mathrm{sgn}(h^0_{ii} - h^0_{kk}) |h_{ik}|^2 = 0. \tag{A.5}$$

From this equation follows that *either* the eigen states $|\nu_i\rangle$ and $|\nu_k\rangle$ are degenerate, *i.e.* they belong to the same block, *or* $h_{ik}(\ell = \infty) = 0$, *i.e.* matrix elements linking different blocks vanish. Hence block diagonality is achieved and the number of energy quanta given by H_0 is conserved

$$\lim_{\ell \to \infty} [H_0, H(\ell)] = 0. \tag{A.6}$$

This concludes the formal proof.

To restrict the argument at one stage to finite clusters does not constitute a real restriction for the series expansion in any finite order. The linked cluster theorem tells us that any finite order can be found from an appropriate finite cluster.

In practice, the important issue is whether the physics remains the same on variation of the expansion parameter λ. In our example of dimerized chains the expansion makes sense as long as the gap does not close. In other words, those situations are accessible which can be linked continuously to the dimer limit by gapped systems. Gapless situations can only be described if they are the limit of gapped systems linked to the dimer limit.

Appendix B: Coefficients of the effective Hamiltonian

In the following tables the coefficients $C(\mathbf{m})$ of the effective Hamiltonian (25) are given up to sixth order inclusively. Order 7 to 10 will be available electronically[1].

---

[1]
at `www.thp.uni-koeln.de/~ck/`
or `www.thp.uni-koeln.de/~gu/`
or `www.edpsciences.org`

m	$C(\mathbf{m})$
$\vert\mathbf{m}\vert = 1$	
0	1
$\vert\mathbf{m}\vert = 2$	
1-1	1
2-2	1/2
$\vert\mathbf{m}\vert = 3$	
01-1	−1/2
02-2	−1/8
10-1	1
11-2	1/2
1-21	−1
20-2	1/4
$\vert\mathbf{m}\vert = 4$	
001-1	1/4
002-2	1/32
010-1	−1
011-2	−3/8
01-21	1/4
01-10	1/2
020-2	−1/8
02-20	1/16
02-1-1	−3/8
100-1	1
101-2	1/2
10-21	−1
110-2	1/4
11-1-1	1/2
12-2-1	1/3
12-1-2	1/6
1-22-1	−1
1-2-12	1/2
1-11-1	−1
1-12-2	−3/8
1-1-22	1/8
200-2	1/8
21-1-2	1/12
22-2-2	1/16
2-22-2	−1/8
2-11-2	1/4
$\vert\mathbf{m}\vert = 5$	
0001-1	−1/8
0002-2	−1/128
0010-1	3/4
0011-2	7/32
001-21	−5/16
001-10	−3/8
0020-2	3/64
002-20	−3/128
002-1-1	7/32
0100-1	−3/2
0101-2	−5/8
010-21	7/8
010-10	3/2
0110-2	−1/4
011-20	7/16
011-1-1	−5/8
012-2-1	−7/18
012-1-2	−11/72
01-201	1/8
01-210	−3/8
01-22-1	1/2
01-2-12	−1/24
01-11-1	9/8
01-12-2	35/96
01-1-22	−19/96
01-1-11	−3/8
0200-2	−3/32
020-20	3/32
020-1-1	−1/4
021-2-1	−11/72
021-1-2	−1/18
022-2-2	−5/128
02-21-1	7/24
02-22-2	9/128
02-2-22	−3/128
02-2-11	−1/12
02-10-1	−5/8
02-11-2	−1/4
02-1-21	7/24
1000-1	1
1001-2	1/2
100-21	−1
1010-2	1/4
101-1-1	1/2
102-2-1	1/3
102-1-2	1/6
10-201	1
10-22-1	−1
10-2-12	1/2
10-11-1	−3/2
10-12-2	−5/8
10-1-22	3/8
10-1-11	1/2
1100-2	1/8
110-1-1	1/4
111-2-1	1/6
111-1-2	1/12
112-2-2	1/16
11-21-1	−5/8
11-22-2	−1/4
11-2-22	1/8
11-2-11	1/8
11-11-2	1/4
11-1-21	−1/2
120-2-1	1/9
120-1-2	1/18
121-2-2	1/24
12-21-2	1/6
12-2-21	−1/3
12-10-2	1/12
1-202-1	1
1-20-12	−1/2
1-211-1	1/4
1-212-2	0
1-21-22	1/4
1-21-11	3/4
1-221-2	−1/2
1-22-21	1
1-2-212	−1/6
1-2-102	−1/4
1-101-1	3/4
1-102-2	7/32
1-10-22	−3/32
1-10-11	−1/4
1-111-2	−5/8
1-120-2	−1/4
1-1-202	0
1-1-1-12	1/8
2000-2	1/16
201-1-2	1/24
202-2-2	1/32
20-22-2	−3/32
20-2-22	1/32
20-11-2	1/8
210-1-2	1/36
211-2-2	1/48
21-21-2	1/12
220-2-2	1/64
2-202-2	3/64
2-20-22	−1/64
2-211-2	−1/4
2-2-1-12	1/8
2-101-2	1/4
2-1-2-12	1/4
$\vert\mathbf{m}\vert = 6$	
00001-1	1/16
00002-2	1/512
00010-1	−1/2
00011-2	−15/128
0001-21	5/64
0001-10	1/4
00020-2	−1/64
0002-20	1/128
0002-1-1	−15/128
00100-1	3/2
00101-2	17/32
0010-21	−3/4
0010-10	−3/2
00110-2	11/64
0011-20	−45/128
0011-1-1	17/32
0012-2-1	17/54
0012-1-2	85/864
001-201	1/2
001-210	1/64
001-22-1	−13/24
001-2-12	53/288
001-100	3/8
001-11-1	−29/32
001-12-2	−301/1152
001-1-22	179/1152
001-1-11	7/32
00200-2	3/64
0020-20	−3/64
0020-1-1	11/64
0021-2-1	85/864
0021-1-2	43/1728
0022-2-2	17/1024
002-200	3/256
002-21-1	−197/1152
002-22-2	−29/1024
002-2-22	7/1024
002-2-11	−23/1152
002-10-1	17/32
002-11-2	11/64
002-1-21	−65/288
002-1-10	−45/128
01000-1	−2
01001-2	−7/8
0100-21	23/16
0100-10	3
01010-2	−3/8
0101-20	17/16
0101-1-1	−7/8
0102-2-1	−5/9
0102-1-2	−17/72
010-201	−5/8
010-210	−3/4
010-22-1	9/8
010-2-12	−7/18
010-11-1	39/16
010-12-2	269/288
010-1-22	−181/288
010-1-11	−17/16
01100-2	−5/32
0110-20	11/32
0110-1-1	−3/8
0111-2-1	−17/72
0111-1-2	−7/72
0112-2-2	−9/128
011-21-1	5/6
011-22-2	113/384
011-2-22	−67/384
011-2-11	−7/24
011-10-1	−7/8
011-11-2	−3/8
011-1-21	7/12
011-1-10	17/16
0120-2-1	−4/27
0120-1-2	−13/216
0121-2-2	−25/576
012-20-1	−5/9
012-21-2	−17/72
012-2-21	103/288
012-2-10	17/27
012-10-2	−7/72
012-1-20	85/432
012-1-1-1	−17/72
01-2001	−9/16
01-202-1	0
01-20-12	−1/6
01-211-1	−2/3
01-212-2	−15/64
01-21-22	37/192
01-21-11	13/24
01-220-1	7/8
01-221-2	1/3
01-22-21	−5/16
01-22-10	−11/12
01-2-212	−1/144
01-2-221	−25/288
01-2-102	−1/36
01-2-111	−1/6
01-2-120	31/144
01-101-1	−1
01-102-2	−329/1152
01-10-22	53/384
01-10-11	3/16
01-110-1	33/16
01-111-2	73/96
01-11-21	−49/48
01-11-10	−27/16
01-120-2	151/576
01-12-20	−149/384
01-12-1-1	73/96
01-1-202	47/576
01-1-211	17/96
01-1-220	113/1152
01-1-101	7/16
01-1-12-1	−31/48
01-1-1-12	17/96
02000-2	−1/16
0200-20	3/32
0200-1-1	−5/32
0201-2-1	−7/72
0201-1-2	−11/288
0202-2-2	−7/256
020-21-1	73/288
020-22-2	39/512
020-2-22	−17/512
020-2-11	−17/288
020-10-1	−3/8
020-11-2	−5/32
020-1-21	2/9
0210-2-1	−13/216
0210-1-2	−5/216
0211-2-2	−19/1152
021-20-1	−17/72
021-21-2	−7/72
021-2-21	19/144
021-10-2	−11/288
021-1-20	43/864
021-1-1-1	−7/72
0220-2-2	−3/256
022-20-2	−7/256
022-2-20	17/512
022-2-1-1	−9/128
022-1-2-1	−25/576
022-1-1-2	−19/1152
02-201-1	−211/1152
02-202-2	−1/32
02-20-22	3/512
02-20-11	−7/384
02-210-1	95/144
02-211-2	85/384
02-21-21	−53/192
02-220-2	33/512
02-22-20	−27/512
02-22-1-1	85/384
02-2-202	7/512
02-2-211	23/384
02-2-101	31/144
02-2-12-1	−11/64
02-2-1-12	23/384
02-100-1	−7/8
02-101-2	−3/8
02-10-21	7/12
02-110-2	−5/32
02-11-20	11/32
02-11-1-1	−3/8
02-12-2-1	−17/72
02-12-1-2	−7/72
02-1-201	−5/36
02-1-22-1	5/12
02-1-2-12	−11/96
02-1-11-1	5/6
02-1-12-2	113/384
02-1-1-22	−67/384
02-1-1-11	−7/24
10000-1	1
10001-2	1/2
1000-21	−1
10010-2	1/4
1001-1-1	1/2
1002-2-1	1/3
1002-1-2	1/6
100-201	1
100-22-1	−1
100-2-12	1/2
100-11-1	−2
100-12-2	−7/8
100-1-22	5/8
100-1-11	1
10100-2	1/8
1010-1-1	1/4
1011-2-1	1/6
1011-1-2	1/12
1012-2-2	1/16
101-21-1	−7/8
101-22-2	−3/8
101-2-22	1/4
101-2-11	3/8
101-10-1	1/2
101-11-2	1/4
101-1-21	−1/2
1020-2-1	1/9
1020-1-2	1/18
1021-2-2	1/24
102-20-1	1/3
102-21-2	1/6
102-2-21	−1/3
102-10-2	1/12
102-1-1-1	1/6
10-202-1	1
10-20-12	−1/2
10-211-1	5/8
10-212-2	3/16
10-21-22	1/16
10-21-11	3/8
10-220-1	−1
10-221-2	−1/2
10-22-21	1
10-2-212	−1/6
10-2-221	−1/3
10-2-102	−1/4
10-2-111	−1/2
10-101-1	3/2
10-102-2	17/32
10-10-22	−9/32
10-10-11	−1/2
10-110-1	−2
10-111-2	−7/8
10-11-21	5/4
10-120-2	−3/8
10-12-1-1	−7/8
10-1-202	−1/8
10-1-211	−1/8
10-1-12-1	3/4
10-1-1-12	−1/8
11000-2	1/16
1100-1-1	1/8
1101-2-1	1/12
1101-1-2	1/24
1102-2-2	1/32
110-21-1	−3/8
110-22-2	−5/32
110-2-22	3/32
110-2-11	1/8
110-11-2	1/8
110-1-21	−1/4
1110-2-1	1/18
1110-1-2	1/36
1111-2-2	1/48
111-21-2	1/12
111-2-21	−1/6
111-10-2	1/24
111-1-1-1	1/12
1120-2-2	1/64
112-20-2	1/32
112-2-1-1	1/16
112-1-2-1	1/24
112-1-1-2	1/48
11-201-1	17/32
11-202-2	11/64
11-20-22	−5/64
11-20-11	−5/32
11-211-2	−3/8
11-21-21	1/2
11-220-2	−5/32
11-22-1-1	−3/8
11-2-202	−1/32
11-2-12-1	1/4
11-101-2	1/4
11-10-21	−1/2
11-110-2	1/8
11-11-1-1	1/4
11-12-2-1	1/6
11-12-1-2	1/12
11-1-22-1	−1/2
11-1-2-12	1/4
11-1-11-1	−7/8
11-1-12-2	−3/8
11-1-1-22	1/4
11-1-1-11	3/8
1200-2-1	1/27
1200-1-2	1/54
1201-2-2	1/72
120-21-2	1/18
120-2-21	−1/9
120-10-2	1/36
1210-2-2	1/96
121-20-2	1/48
121-1-2-1	1/36
121-1-1-2	1/72
122-2-2-1	1/45
122-2-1-2	1/90
122-1-2-2	1/120
12-201-2	1/6
12-20-21	−1/3
12-210-2	1/12
12-22-2-1	1/9
12-22-1-2	1/18
12-2-22-1	−1/3
12-2-2-12	1/6
12-2-11-1	−5/9
12-2-12-2	−17/72
12-2-1-22	11/72
12-2-1-11	2/9
12-100-2	1/24
12-11-2-1	1/18
12-11-1-2	1/36
12-12-2-2	1/48
12-1-21-1	−17/72
12-1-22-2	−7/72
12-1-2-22	1/18
12-1-2-11	5/72
12-1-11-2	1/12
12-1-1-21	−1/6
1-2002-1	−1
1-200-12	1/2
1-2011-1	3/8
1-2012-2	5/16
1-201-22	−9/16
1-201-11	−11/8
1-2021-2	1/2
1-202-21	−1
1-20-212	1/6
1-20-102	1/4
1-2101-1	−7/16
1-2102-2	−5/32
1-210-22	7/32
1-210-11	11/16
1-2111-2	1/4
1-2120-2	1/16
1-21-202	−3/16
1-21-12-1	1/2
1-21-1-12	−1/2
1-2201-2	−1/2
1-2210-2	−1/4
1-222-1-2	−1/6
1-22-22-1	1
1-22-2-12	−1/2
1-22-11-1	1
1-22-12-2	3/8
1-22-1-22	−1/8
1-22-1-11	0
1-2-2012	1/18
1-2-2102	1/12
1-2-222-1	−1/3
1-2-22-12	1/6
1-2-2-122	1/24
1-2-1002	1/8
1-2-112-1	−1/2
1-2-11-12	1/4
1-2-121-1	1/24
1-2-122-2	1/12
1-2-12-22	−5/24
1-2-12-11	−13/24
1-2-1-222	1/16
1-2-1-112	1/12
1-1001-1	−1/2
1-1002-2	−15/128
1-100-22	5/128
1-1011-2	17/32
1-1020-2	11/64

$\mathbf{m}$	$C(\mathbf{m})$
$\lvert\mathbf{m}\rvert = 6$	
1-10-202	3/64
1-10-1-12	5/32
1-1101-2	−7/8
1-1110-2	−3/8
1-112-1-2	−17/72
1-11-2-12	−7/24
1-11-11-1	2
1-11-12-2	71/96
1-11-1-22	−43/96
1-11-1-11	−3/4
1-1200-2	−5/32
1-121-1-2	−7/72
1-122-2-2	−9/128
1-12-21-1	31/48
1-12-22-2	83/384

$\mathbf{m}$	$C(\mathbf{m})$
$\lvert\mathbf{m}\rvert = 6$	
1-12-2-22	−41/384
1-12-2-11	−3/16
1-12-11-2	−3/8
1-1-2002	−1/32
1-1-21-12	−1/8
1-1-221-1	−11/48
1-1-222-2	−25/384
1-1-22-22	19/384
1-1-2-222	−1/128
1-1-2-112	−1/72
1-1-10-12	−3/8
1-1-111-1	−1/2
1-1-112-2	−19/96
1-1-11-22	23/96
1-1-121-2	5/24

$\mathbf{m}$	$C(\mathbf{m})$
$\lvert\mathbf{m}\rvert = 6$	
1-1-1-212	−5/72
1-1-1-102	−1/8
20000-2	1/32
2001-1-2	1/48
2002-2-2	1/64
200-22-2	−1/16
200-2-22	1/32
200-11-2	1/16
2010-1-2	1/72
2011-2-2	1/96
201-21-2	1/24
201-10-2	1/48
2020-2-2	1/128
202-20-2	1/64
202-1-1-2	1/96

$\mathbf{m}$	$C(\mathbf{m})$
$\lvert\mathbf{m}\rvert = 6$	
20-202-2	3/64
20-20-22	−1/64
20-211-2	−5/32
20-220-2	−1/16
20-2-1-12	1/32
20-101-2	1/8
20-110-2	1/16
20-12-1-2	1/24
20-1-2-12	1/8
20-1-12-2	−5/32
20-1-1-22	3/32
2100-1-2	1/108
2101-2-2	1/144
210-21-2	1/36
2110-2-2	1/192

$\mathbf{m}$	$C(\mathbf{m})$
$\lvert\mathbf{m}\rvert = 6$	
211-1-1-2	1/144
212-2-1-2	1/180
212-1-2-2	1/240
21-201-2	1/12
21-22-1-2	1/36
21-2-2-12	1/12
21-2-12-2	−7/72
21-2-1-22	1/18
21-11-1-2	1/72
21-12-2-2	1/96
21-1-22-2	−11/288
21-1-2-22	5/288
21-1-11-2	1/24
2200-2-2	1/256
221-1-2-2	1/320

$\mathbf{m}$	$C(\mathbf{m})$
$\lvert\mathbf{m}\rvert = 6$	
222-2-2-2	1/384
22-22-2-2	1/128
22-2-22-2	−7/256
22-2-2-22	3/256
22-2-11-2	1/32
22-11-2-2	1/192
22-1-21-2	1/48
2-2002-2	−1/64
2-2011-2	11/64
2-20-1-12	5/64
2-2101-2	−3/8
2-21-2-12	−1/12
2-21-12-2	49/192
2-21-1-22	−9/64
2-22-22-2	1/16

$\mathbf{m}$	$C(\mathbf{m})$
$\lvert\mathbf{m}\rvert = 6$	
2-22-2-22	−3/128
2-22-11-2	−5/32
2-2-21-12	−3/32
2-2-222-2	−1/64
2-2-10-12	−1/4
2-2-112-2	−17/192
2-2-121-2	1/24
2-1001-2	1/4
2-10-2-12	1/4
2-11-11-2	1/8
2-12-21-2	1/12
2-1-221-2	−1/4
2-1-111-2	−3/8

Appendix C: Effective hopping elements for the spin chain

In the following the effective hopping elements as they appear in equation (38) are given up to order 6. The effective hopping elements up to order 10 will be provided electronically. We substituted $\overline{\alpha} = 1 - 2\alpha$ and $\overline{\lambda} = \frac{1}{4}\lambda$.

$$\begin{aligned}
a_0 - E_0 = {} & 1 - \left(4 - 3\overline{\alpha}^2\right)\overline{\lambda}^2 - \left(8 - 8\overline{\alpha} - 6\overline{\alpha}^2 + 3\overline{\alpha}^3\right)\overline{\lambda}^3 - \left(2 - 24\overline{\alpha} + 5\overline{\alpha}^2 + 8\overline{\alpha}^3 + \frac{13}{4}\overline{\alpha}^4\right)\overline{\lambda}^4 \\
& + \left(56 - 82\overline{\alpha} - 22\overline{\alpha}^2 + 55\overline{\alpha}^3 - 39\overline{\alpha}^4 + 20\overline{\alpha}^5\right)\overline{\lambda}^5 \\
& + \left(\frac{367}{3} - \frac{7328}{9}\overline{\alpha} + \frac{22976}{27}\overline{\alpha}^2 + \frac{6442}{27}\overline{\alpha}^3 - \frac{28895}{54}\overline{\alpha}^4 + 193\overline{\alpha}^5 - 32\overline{\alpha}^6\right)\overline{\lambda}^6 \\
a_1 = {} & -2\overline{\alpha}\overline{\lambda} - 4\overline{\lambda}^2 - \left(8 - 8\overline{\alpha} - 2\overline{\alpha}^3\right)\overline{\lambda}^3 + \left(4 + 20\overline{\alpha} - 24\overline{\alpha}^2 + 10\overline{\alpha}^3 - 5\overline{\alpha}^4\right)\overline{\lambda}^4 \\
& + \left(92 - \frac{499}{3}\overline{\alpha} - \frac{164}{3}\overline{\alpha}^2 + 152\overline{\alpha}^3 - 47\overline{\alpha}^4 + \frac{13}{2}\overline{\alpha}^5\right)\overline{\lambda}^5 \\
& + \left(\frac{532}{3} - \frac{11906}{9}\overline{\alpha} + \frac{11960}{9}\overline{\alpha}^2 + \frac{1648}{3}\overline{\alpha}^3 - \frac{41357}{54}\overline{\alpha}^4 + 85\overline{\alpha}^5 + 6\overline{\alpha}^6\right)\overline{\lambda}^6 \\
a_2 = {} & -\overline{\alpha}^2\overline{\lambda}^2 - \left(4\overline{\alpha}^2 - 2\overline{\alpha}^3\right)\overline{\lambda}^3 + \left(6 - 4\overline{\alpha} - 23\overline{\alpha}^2 + 14\overline{\alpha}^3 - \frac{1}{2}\overline{\alpha}^4\right)\overline{\lambda}^4 \\
& + \left(36 - \frac{272}{3}\overline{\alpha} - \frac{220}{3}\overline{\alpha}^2 + \frac{1150}{9}\overline{\alpha}^3 - 9\overline{\alpha}^4 - \frac{13}{2}\overline{\alpha}^5\right)\overline{\lambda}^5 \\
& + \left(\frac{107}{3} - \frac{1630}{3}\overline{\alpha} + \frac{1126}{3}\overline{\alpha}^2 + \frac{5102}{9}\overline{\alpha}^3 - \frac{13205}{36}\overline{\alpha}^4 - 59\overline{\alpha}^5 + 11\overline{\alpha}^6\right)\overline{\lambda}^6 \\
a_3 = {} & -\overline{\alpha}^3\overline{\lambda}^3 - \left(\frac{10}{3}\overline{\alpha}^2 + 4\overline{\alpha}^3 - 2\overline{\alpha}^4\right)\overline{\lambda}^4 - \left(\frac{19}{3}\overline{\alpha} + 20\overline{\alpha}^2 - \frac{10}{3}\overline{\alpha}^3 - 11\overline{\alpha}^4 - 3\overline{\alpha}^5\right)\overline{\lambda}^5 \\
& - \left(\frac{58}{3} + \frac{104}{3}\overline{\alpha} - \frac{224}{9}\overline{\alpha}^2 - 63\overline{\alpha}^3 + \frac{103}{2}\overline{\alpha}^4 - \frac{57}{2}\overline{\alpha}^5 + \frac{81}{4}\overline{\alpha}^6\right)\overline{\lambda}^6 \\
a_4 = {} & -\frac{5}{4}\overline{\alpha}^4\overline{\lambda}^4 - \left(\frac{40}{9}\overline{\alpha}^3 + 6\overline{\alpha}^4 - 3\overline{\alpha}^5\right)\overline{\lambda}^5 + \left(\frac{11}{3}\overline{\alpha}^2 - \frac{827}{27}\overline{\alpha}^3 - \frac{1127}{36}\overline{\alpha}^4 + \frac{91}{4}\overline{\alpha}^5 + \frac{73}{16}\overline{\alpha}^6\right)\overline{\lambda}^6 \\
a_5 = {} & -\frac{7}{4}\overline{\alpha}^5\overline{\lambda}^5 - \left(\frac{497}{54}\overline{\alpha}^4 + 10\overline{\alpha}^5 - 5\overline{\alpha}^6\right)\overline{\lambda}^6 \\
a_6 = {} & -\frac{21}{8}\overline{\alpha}^6\overline{\lambda}^6.
\end{aligned}$$

References

1. J.W. Bray, L.V. Interrante, I.C. Jacobs, J.C. Bonner, in *Extended Linear Chain Compounds*, edited by J.S. Miller (Plenum Press, New York, 1983), Vol. 3, p. 353.
2. J. Riera, A. Dobry, Phys. Rev. B **51**, 16098 (1995).
3. G. Castilla, S. Chakravarty, V.J. Emery, Phys. Rev. Lett. **75**, 1823 (1995).
4. K. Fabricius *et al.*, Phys. Rev. B **57**, 1102 (1998).
5. G. Chaboussant *et al.*, Phys. Rev. B **55**, 3046 (1997).
6. A.W. Garrett *et al.*, Phys. Rev. Lett. **79**, 745 (1997).
7. G.S. Uhrig, B. Normand, Phys. Rev. B **58**, R14705 (1998).
8. J. Stein, J. Stat. Phys. **88**, 487 (1997).
9. A.H. MacDonald, S.M. Girvin, D. Yoshioka, Phys. Rev. B **37**, 9753 (1988).
10. F.J. Wegner, Ann. Phys. **3**, 77 (1994).
11. S.K. Kehrein, A. Mielke, P. Neu, Z. Phys. B **99**, 269 (1996).
12. S.K. Kehrein, A. Mielke, Ann. Phys. **252**, 1 (1996).
13. S.D. Głazeck, K.G. Wilson, Phys. Rev. D **48**, 5863 (1993); *ibid.* **49**, 4214 (1994).
14. A. Mielke, Eur. Phys. J. B **5**, 605 (1998).
15. M.C. Cross, D.S. Fisher, Phys. Rev. B **19**, 402 (1979).
16. G.S. Uhrig, H.J. Schulz, Phys. Rev. B **54**, R9624 (1996); *ibid.* **58**, 2900 (1998).
17. J.L. Black, V.J. Emery, Phys. Rev. B **23**, 429 (1981).
18. I. Affleck, D. Gepner, H.J. Schulz, T. Ziman, J. Phys. A **22**, 511 (1989).
19. S. Eggert, Phys. Rev. B **54**, R9612 (1996).
20. T. Barnes, J. Riera, D.A. Tennant, `cond-mat/9801224`.
21. M.P. Gelfand, R.R.P. Singh, D.A. Huse, J. Stat. Phys. **59**, 1093 (1990).
22. Z. Weihong, V. Kotov, J. Oitmaa, Phys. Rev. B **57**, 11439 (1998).
23. G.S. Uhrig, F. Schönfeld, M. Laukamp, E. Dagotto, Eur. Phys. J. B **7**, 67 (1999).
24. R. Chitra *et al.*, Phys. Rev. B **52**, 6581 (1995).
25. S.R. White, I. Affleck, Phys. Rev. B **54**, 9862 (1996).
26. F.D.M. Haldane, Phys. Rev. B **25**, 4925 (1982).
27. L.P. Kadanoff, Phys. Rev. B **22**, 1405 (1980).
28. J. des Cloizeaux, J.J. Pearson, Phys. Rev. **128**, 2131 (1962).
29. W.J. Caspers, W. Magnus, Phys. Lett. A **88**, 103 (1982).
30. E. Müller-Hartmann, G.S. Uhrig, in preparation.
31. B.S. Shastry, B. Sutherland, Phys. Rev. Lett. **47**, 964 (1981).
32. W.J. Caspers, K.M. Emmett, W. Magnus, J. Phys. A **88**, 103 (1982).
33. S. Brehmer, A.K. Kolezhuk, H. Mikeska, U. Neugebauer, J. Phys. Cond. Matter **10**, 1103 (1998).
34. C. Domb, J.L. Lebowitz, *Phase Transitions and Critical Phenomena*, (Academic Press, New York, 1989), Vol. 13.
35. G.S. Uhrig, Phys. Rev. Lett. **79**, 163 (1997).
36. D. Cremers, A. Mielke, Physica D **126**, 123 (1999).